Division of Pharmaceutical Technology
Faculty of Pharmacy
University of Helsinki
Finland

Investigating physical properties of solid dosage forms during pharmaceutical processing

Process analytical applications of vibrational spectroscopy

Meike Römer

ACADEMIC DISSERTATION

To be presented, with the permission of the Faculty of Pharmacy of the University of Helsinki, for public examination in auditorium 2041, Biocenter 2 (Viikinkaari 5E), on August 4th 2008, at 12 noon.

Helsinki 2008

Supervisors: Dr. Clare Strachan
Centre for Drug Research (CDR)
Faculty of Pharmacy
University of Helsinki
Finland

Docent Jyrki Heinämäki
Division of Pharmaceutical Technology
Faculty of Pharmacy
University of Helsinki
Finland

Professor Jouko Yliruusi
Division of Pharmaceutical Technology
Faculty of Pharmacy
University of Helsinki
Finland

Reviewers: Dr. Katherine A. Bakeev
GlaxoSmithKline
King of Prussia - Pennsylvania
USA

Dr. Manel Alcalà-Bernàrdez
Department of Chemistry
Faculty of Arts and Science
University of Puerto Rico - Mayagüez
Puerto Rico

Opponent: Professor Chris Vervaet
Laboratory of Pharmaceutical Technology
Faculty of Pharmaceutical Sciences
Ghent University
Belgium

ISBN 978-952-10-4753-4 (paperback)
ISBN 978-952-10-4754-1 (PDF, http://ethesis.helsinki.fi)
ISSN 1795-7079

Helsinki University Print
Helsinki 2008

Abstract

Römer, M. (2008) Investigating physical properties of solid dosage forms during pharmaceutical processing – Process analytical applications of vibrational spectroscopy.

Dissertationes bioscientiarum molecularium Universitatis Helsingiensis in Viikki, 30/2008, pp. 48.
ISBN 978-952-10-4753-4 (paperback), ISBN 978-952-10-4754-1 (PDF), ISSN 1795-7079

In order to improve and continuously develop the quality of pharmaceutical products, the process analytical technology (PAT) framework has been adopted by the US Food and Drug Administration. One of the aims of PAT is to identify critical process parameters and their effect on the quality of the final product. Real time analysis of the process data enables better control of the processes to obtain a high quality product.

The main purpose of this work was to monitor crucial pharmaceutical unit operations (from blending to coating) and to examine the effect of processing on solid-state transformations and physical properties. The tools used were near-infrared (NIR) and Raman spectroscopy combined with multivariate data analysis, as well as X-ray powder diffraction (XRPD) and terahertz pulsed imaging (TPI).

To detect process-induced transformations in active pharmaceutical ingredients (APIs), samples were taken after blending, granulation, extrusion, spheronisation, and drying. These samples were monitored by XRPD, Raman, and NIR spectroscopy showing hydrate formation in the case of theophylline and nitrofurantoin. For erythromycin dihydrate formation of the isomorphic dehydrate was critical. Thus, the main focus was on the drying process. NIR spectroscopy was applied in-line during a fluid-bed drying process. Multivariate data analysis (principal component analysis) enabled detection of the dehydrate formation at temperatures above 45°C.

Furthermore, a small-scale rotating plate device was tested to provide an insight into film coating. The process was monitored using NIR spectroscopy. A calibration model, using partial least squares regression, was set up and applied to data obtained by in-line NIR measurements of a coating drum process. The predicted coating thickness agreed with the measured coating thickness. For investigating the quality of film coatings TPI was used to create a 3-D image of a coated tablet. With this technique it was possible to determine coating layer thickness, distribution, reproducibility, and uniformity. In addition, it was possible to localise defects of either the coating or the tablet.

It can be concluded from this work that the applied techniques increased the understanding of physico-chemical properties of drugs and drug products during and after processing. They additionally provided useful information to improve and verify the quality of pharmaceutical dosage forms.

Acknowledgements

The present work was carried out in the Division of Pharmaceutical Technology, Faculty of Pharmacy, University of Helsinki.

My thanks goes to all people involved in this work, especially my supervisor, Professor Jouko Yliruusi, for his guidance and constant support throughout all these years. Without his persistence I would never have considered doing a PhD, after all. I would also like to thank my co-supervisors Jyrki Heinämäki, Clare Strachan, and, of course, Jukka Rantanen for their patience with me and for their useful advice.

All my co-authors are acknowledged for their scientific contributions and their friendship. Special thanks goes to Niklas Sandler and to my co-worker Louise Ho. Working with Louise has been enlightening and challenging at the same time, due to the project being coordinated over such a distance, consequently, the developers of Skype should be acknowledged here, too. Maike Stiers, Alex Bunker, and Andrea Heinz have generously improved my work life with relaxing coffee breaks.

I would also like to express my gratitude to Katherine A. Bakeev for her support, guidance and belief in me. Manel Alcalà is thanked for reviewing this thesis and for the pleasure of witnessing his rise to the best entertainer Memphis has ever seen. Jeremy Shaver and Frank Westad are acknowledged for their friendship, for sharing their knowledge of chemometrics with me, and for cheering me up every time I wanted to throw in the towel.

Last but not least, I would like to thank my parents for just everything. There is no way of describing how much they have helped me, especially Conni for being there every time Malin and I needed her. Malin, of course, for reminding me that there is more in life than a job, for strengthening my nerves and enriching my life with joy, a lot of chaos and consequently a lot of laughter.

Helsinki, August 2008

Table of contents

List of original publications

This thesis is based on the following publications:

I Sandler N., Rantanen J., Heinämäki J., **Römer M**., Marvola M., Yliruusi J. (2005) Pellet manufacturing by extrusion-spheronization using process analytical technology. *AAPS PharmSciTech*. **6**(2): E174-E183.

II **Römer M.**, Heinämäki J., Miroshnyk I., Sandler N., Rantanen J., Yliruusi J. (2007) Phase transformations of erythromycin A dihydrate during pelletisation and drying. *European Journal of Pharmaceutics and Biopharmaceutics* **67**(1): 246-252.

III **Römer M.**, Heinämäki J., Miroshnyk I., Kivikero N., Sandler N., Rantanen J., Yliruusi J. (2008) Phase transformation of erythromycin A dihydrate during fluid bed drying. *Journal of Pharmaceutical Sciences* **doi** 10.1002/jps.21272.

IV **Römer M.**, Heinämäki J., Strachan C. J., Sandler N., Yliruusi J. Prediction of tablet film coating thickness using a rotating plate coating system and NIR spectroscopy. *AAPS PharmSciTech*. Submitted.

V Ho L., Müller R., **Römer M.**, Gordon K. C., Heinämäki J., Kleinebudde P., Pepper M., Rades T., Shen Y. C., Strachan C. J., Taday P. F., Zeitler J. A. (2007) Analysis of sustained-release tablet film coats using terahertz pulsed imaging. *Journal of Controlled Release* **119**(3): 253-261.

The publications are referred to in the text by their Roman numerals. Reprinted with permission from the publishers.

Abbreviations

API	active pharmaceutical ingredient
ATR	attenuated total reflection
cGMP	current Good Manufacturing Practice
coop-reorg	cooperative-reorganisation
coop-cryst	cooperative-crystallisation
coop-disorg	cooperative-disorganisation
CSD	Cambridge Structural Database
destr-disorg	destructive-disorganisation
destr-cryst	destructive-crystallisation
DRIFT	diffuse reflectance infrared Fourier transform
DSC	differential scanning calorimetry
EM	erythromycin
EMEA	European Agency for Evaluation of Medical Products
FDA	Food and Drug Administration
FT-IR	Fourier-transform infrared
HPLC	high performance liquid chromatography
ICH	International Conference on Harmonisation
LV	latent variable
MC	mean centering
NF	nitrofurantoin
NIR	near-infrared
NMR	nuclear magnetic resonance
PAT	process analytical technology
PCA	principal component analysis
PC	principal component
Ph.Eur.	European Pharmacopoeia
PITs	process-induced transformations
PLS	partial least squares
PRESS	predicted error sum of squares
RI	refractive index
RMSECV	root mean squared error of cross-validation
SNV	standard normal variate
TP	theophylline
TPS	terahertz pulsed spectroscopy
TPI	terahertz pulsed imaging
XRPD	X-ray powder diffraction

1. Introduction

Approaches to investigate the manufacturing and processing of pharmaceutical formulations have gained more attention within recent years. The aims are to both, find new ways of processing active pharmaceutical ingredients (APIs) and excipients, and to better understand the underlying principles of currently used processes and induced transformations.

During manufacturing the materials being processed are subjected to mechanical and/or thermal stresses and are often exposed to solvents, such as water. These stresses may induce process-induced transformations (PITs) and thus affect the quality and properties of the final product. In order to determine critical steps during manufacturing in which these PITs take place, the physico-chemical properties of APIs and excipients should be taken into consideration, as well as the knowledge about the kinds of stresses applied during the different steps. This knowledge should give clues as to which processes should be monitored closely for potential PITs. Nevertheless, most PITs are difficult to predict and model (Morris et al. 2001). Thus, it has proven useful to first take samples after every processing step and examine these samples with easily applicable at-line techniques. In addition to monitoring solid-state changes, other physical properties, for example, particle size, particle size distribution, and change of sample texture (Norris & Williams 1983) should be closely examined during processing. Measuring theses properties throughout the process, rather than relying solely on end-product testing, will better ensure the quality of the product.

To identify and monitor these critical steps process analytical technology (PAT) is used, which is defined by the US Food and Drug Administration (FDA) as follows: “PAT is a system for designing, analyzing, and controlling manufacturing through timely measurements […] with the final goal of ensuring final product quality (FDA 2004a)”. PAT analysis can be done either in-line (sample not removed or diverted from the process), on-line (sample diverted and returned to the process), at-line (sample removed and analysed in the process area) or off-line (sample removed from process area). The concept combines four main areas: monitoring, supervision, control and diagnosis (Rodrigues et al. 2006). It has come into focus in the pharmaceutical industry as a promising concept to increase product quality while lowering the manufacturing costs and reducing the time to market for newly developed pharmaceutical products.

Spectroscopic techniques, such as mid-infrared, near-infrared (NIR), and Raman spectroscopy, are widely used for real-time measurements and quality control. NIR spectroscopy has become a synonym for PAT being already implemented for decades within the agricultural, food and chemical industries. The European Agency for Evaluation of Medical Products (EMEA) has published a detailed guideline on the use of NIR spectroscopy (EMEA 2003). Nevertheless, there are more techniques available for investigating manufacturing processes. In addition to mid-infrared and Raman spectroscopy, terahertz pulsed spectroscopy (TPS) and terahertz pulsed imaging (TPI) are relatively new techniques. Both have shown great potential in the

field of polymorph identification (Strachan et al. 2005) and film coating quality determination (Fitzgerald et al. 2005). In-line measurements are not possible with all techniques they often require labour intensive, time consuming calibration and data processing. But, if applied wisely, such techniques can provide an in depth understanding of a process. X-ray powder diffraction (XRPD) is often used off-line or at-line for identifying solid-state changes of crystalline material, as is differential scanning calorimetry (DSC) for detecting endothermic or exothermic events. Benefits that one can expect from the application of PAT during the different unit operations are presented in Table 1.

Table 1. *Possibilities for monitoring and investigating pharmaceutical unit operations (modified from Bakeev 2003, Rantanen 2007, Räsänen & Sandler 2007).*

Critical quality parameter	Pharmaceutical unit operations	Information obtained by process analytical tools
Qualification, particle size distribution	Raw materials	Raw materials, chemical and physical properties
Yield, purity, degradation	Synthesis	By-products and rate constants, end-point
Polymorphic forms, speed of crystallisation, purity, surface properties, particle size and shape distribution	Crystallisation	Crystallisation progress, important process operating conditions, degree of crystallinity, solid-state transformation → particle design at molecular level
Particle size reduction, phase transitions	Milling	Polymorphic transformations, creation of amorphous material, particle size development
Homogeneity	Mixing	Real time blend uniformity, end-point
Particle size distribution, phase transitions (solvent exposure, thermal and mechanical stress)	Granulation	Particle size, moisture content, phase transitions, end-point
Phase transitions (desolvation, dehydration)	Drying	Dehydration/desolvation process (moisture loss), end-point
Relative density, tensile strength, Young's modulus, phase transitions	Tableting	Physical properties, polymorphic transformations, pressure-induced amorphisation, content uniformity
Coating thickness and uniformity, interaction of coating solution and tablet core material	Tablet coating	Coating time and coating thickness, coating variations and uniformity
Degradation products, identification of counterfeits	Packaging Shelf life	Identification, stability

In this thesis hydrate formation and dehydration behaviour were investigated during blending, pelletisation, and drying. Raman, NIR spectroscopy, and XRPD have been applied to assess the changes in solid-state properties. In-line NIR spectroscopy was used to monitor the dehydration behaviour of pellets containing erythromycin (EM) during fluid-bed drying. The coating process of compacts was investigated and a calibration model using in-line NIR data of a small-scale coating method was applied to determine the coating thickness of tablets during a coating drum process. Furthermore, coating quality parameters of sustained-release coated tablets, such as coating thickness, distribution, and uniformity were determined using TPI.

2. Theory and literature review

2.1. Process analytical technology

With the aim of making pharmaceutical production more efficient and manufacturing higher quality products in which the quality is built in (FDA 2004a), the FDA released a new version of the pharmaceutical current Good Manufacturing Practices (cGMPs) in 2004 (FDA 2004b). To encourage implementation of risk-based approaches they additionally released the PAT guideline as non-binding recommendations. The idea behind this emerged because for various drugs neither the mechanisms of degradation, drug release and absorption nor the effects of production were fully understood. The final aim of PAT is to replace conventional quality assurance and quality control methods with techniques that enable real-time release (FDA 2004a). PAT is certainly not a new concept and has been known as process analytical chemistry (Beebe et al. 1993, Baughman 2005, Workman et al. 2007). Other industries (Workman 1999), including the paper industry (Workman 2001) and food science (Tenhunen et al. 1994, Huang et al. 2008), have used this concept for decades but regulatory burden has delayed such progress in the pharmaceutical industry.

Long before this guideline was published research was conducted to show the benefits of PAT. A review about PAT applications in the pharmaceutical industry, including raw material qualification, moisture content analysis, dehydration of hydrate and solvates during processes was published by Morris et al. (1998). In another study the focus was on complications for solid formulations that arise from their chemical reactivity (Byrn et al. 2001). In this study solid-state changes, as well as oxidation of APIs and incompatibility reactions between drugs and excipients were investigated. The need for monitoring processes and identifying possible solid-state reactions was clearly shown. Investigating the process of crystallisation is also a focus of PAT due to its potential in the detection of polymorphic forms (Févotte et al. 2004). The influence of thermodynamics on the different polymorphic forms can be assessed by monitoring the crystallisation process with different in-line and at-line techniques. Particle size and shape evolution during crystallisation can also be investigated by NIR spectroscopy and image analysis (Yu et al. 2004). The combined information may assist to adjust and improve the control of a crystallisation process.

Zhang et al. (2004) published their results on PITs concluding that the underlying mechanism of the phase transition and critical process parameters are crucial information in designing a rational formulation. Similar conclusions were obtained when examining the processes of melt granulation and tablet coating by NIR spectroscopy and NIR imaging (Roggo et al. 2005). An example of PAT implementation is presented in a study ranging from the feasibility testing of NIR spectroscopy in quantifying the drug content of tablets, to determining tablet hardness and calibration transfer between different kinds of NIR spectrometers (Cogdill et al. 2005 a, b, c).

All this research demonstrates that the necessary information about APIs, excipients, and processes for modelling possible polymorphic forms, PITs, incompatibilities, dissolution profiles, and bioavailability can be obtained using PAT. Not only is knowledge about the optimal physico-chemical and pharmaceutical properties of an API required, but also knowledge of the processes applied and the critical steps associated with physical and chemical changes, so that such changes can be controlled (ICH 1999, ICH 2005, ICH 2007).

2.2. Solid-state transformations during processing

Solid forms can exhibit polymorphism, which can be categorised into true polymorphs, solvates/hydrates (pseudo-polymorphs), isomorphic desolvates/ dehydrates, and amorphous solids. True polymorphs are of the same chemical composition but exhibit different crystalline modifications. Solvates and hydrates are also crystalline but include solvent molecules (water in the case of hydrates) in their crystal lattice. Isomorphic desolvates/dehydrates exhibit only minor structural differences from the solvate/hydrate apart from the lack of solvent molecules. Amorphous material lacks the long-range structural order that crystalline materials possess (Yu et al. 1998).

The different solid states of a substance exhibit different physico-chemical and pharmaceutical properties. This may have an effect on powder flow, tablet hardness, and compressibility during processing. Even after production storage stability, dissolution rate, and bioavailability may differ between the different solid-state forms due to different melting points, densities, dissolution rates, and solubilities (Halebian & McCrone 1969, Grant 1999, Yu et al. 1998). Screening for the polymorphic structure of APIs is required from the regulatory bodies for newly developed drugs, e.g. the International Conference for Harmonisation (ICH 1999). In addition, it offers the possibility to patent polymorphic forms, to study structure-property relationships, and finally to engineer solids with optimised properties (Yu et al. 1998, Zhang et al. 2004).

The formation of true polymorphic structures depends on thermodynamic and kinetic factors. The most common classification for true polymorphs divides them into enantiotropic and monotropic systems (Giron 1995, Halebian & McCrone 1969). In an enantiotropic system different polymorphic forms may coexist in a certain temperature range or convert to a metastable intermediate during transition. The thermodynamically stable form is the form with the lower free energy. Even though the thermodynamically stable form at ambient conditions usually shows preferable process and storage stability, it is not necessarily the preferred form, since the apparent solubility is lower. Forms with the higher thermodynamic activity, on the other hand, possess a more favourable apparent solubility and dissolution rate. In a monotropic system the different polymorphs usually do not coexist. The system converts only in one direction: from the thermodynamically less stable form to the more stable form that has the higher melting point. A metastable form can only occur

through kinetic conversion. Any stress applied to this kind of polymorphic system can yield the stable form (Morris et al. 2001).

To better understand the underlying behaviour of a solid-state system, thermodynamic measurements provide information about the number of phases, the states of aggregation, the stability of the detected phase in relation to temperature and pressure, and the latent heat of transitions (Morris et al. 2001).

Methods to determine thermodynamic properties include differential scanning calorimetry (DSC), thermogravimetric analysis, microcalorimetry, and solution calorimetry (Ph.Eur. 2008a). By measuring the heat flow versus temperature, DSC can detect melting point, heat capacity, heat of fusion/transition, solid-solid phase transitions, as well as the lattice relaxation (Vyazovkin & Dranca 2005). DSC is further able to assess the glass transition temperature (T_g), which characterises amorphous solids. For polymorphic mixes DSC can detect melting point depression and eutectic melting (Hoppu et al. 2007). Solution calorimetry, which measures the heat of solvation, is a sensitive method to detect amorphous solids and quantify the crystalline-amorphous mixtures (Lehto et al. 2006). Amorphous materials usually show an increase in heat of crystallisation and solvation.

Polymorphic forms can also be characterised by microscopy (Mirza et al. 2003), hot stage microscopy (Mirza et al. 2006) or scanning electron microscopy (Aaltonen et al. 2006). Differences can be seen in morphology, refractive indices, and birefringence. Desolvates are characterised by microcrystalline domains and amorphous solids are readily detectable by their lack of birefringence. Often moisture sorption/desorption isotherms can be used to predict storage stability. Thus, the kinetics of dehydration and crystallisation can be assessed by measuring the change of mass versus relative humidity.

Methods to characterise the different solid-state forms on a molecular and particle level are described in Table 2. Stephenson (2005) has published a detailed paper about XRPD, presenting it as a suitable tool for high throughput screening, routinely used for polymorphic screening. In two studies the limit of quantitation of thermal and diffraction methods and vibrational spectroscopy was compared (Giron et al. 2007, Lehto et al. 2006). One of the most frequently used APIs to study polymorphism is carbamazepine. Polymorphic forms have been verified with TPS (Strachan et al. 2005), solid-state nuclear magnetic resonance (NMR) spectroscopy and XRPD (Harris et al. 2005).

A significant effort has been put into stabilising amorphous forms of drugs with low solubility of their crystalline form. Amorphous materials have the advantage of a high apparent solubility, but tend to crystallise during processing or storage. One successful attempt to stabilise amorphous material was to decrease the molecular mobility by annealing (Luthra et al. 2008). Another route to increase the solubility is to stabilise the anhydrous form as a solid dispersion, for example, erythromycin dihydrate in polyethylene glycol 6000 (Mirza et al. 2006). Since water is the most common solvent during pharmaceutical processes, hydrates and dehydrated forms will be discussed in more detail.

Table 2. *Use of diffraction and vibrational spectroscopy to detect solid-state changes (modified from Giron et al. 2004, Yu et al. 1998).*

	Types of polymorphs and information	Data measured	Features
Single crystal XRD	**True polymorphs & solvates:** unit cell parameters, molecular conformation and packing	**Diffractogram:** diffraction intensity as a function either of the scattering angle or scattering vector. Sensitive to long-range order	Difficulties to prepare single crystal (phase purity)
XRPD (Ph.Eur. 2008b)	**True polymorphs & solvates:** diffraction peaks, phase purity, % crystallinity **Isomorphic desolvates:** only subtle changes **Amorphous solids:** no diffraction peaks **Polymorphic mixes:** quantification		Influenced by preferred orientation, variable temperature XRPD, combination with humidity control: studying polymorphic conversions
TPS	**True polymorphs, solvates & isomorphic desolvates:** hydrogen bonding, low energy lattice vibrations, % crystallinity **Amorphous solids:** diffuse response **Polymorphic mixes:** quantification	**Spectra:** dipole moment change, intermolecular vibration and molecular flexing	**Mode:** transmission, specular reflectance, attenuated total reflection (ATR); rapid, sensitive to water vapour, detected modes not yet fully assigned
Solid-state NMR	**True polymorphs:** chemical shifts: phase purity, molecular mobility **Solvates:** solvent resonance peaks, solvent mobility, shifted drug resonances **Isomorphic desolvates:** disappearing solvent resonances, drug resonance shift **Amorphous solids:** peak broadening **Polymorphic mixes:** quantification	**Spectra:** magnetic resonance, sensitivity to electronic environment of specific nuclei	**Variable temperature solid-state-NMR:** molecular dynamics
FT-IR Spectroscopy (Ph.Eur. 2008c)	**True polymorphs:** band shifts **Solvates:** identification of solvent **Amorphous solids:** peak broadening **Polymorphic mixes:** quantification	**Spectra:** dipole moment change, hydrogen bonding	**Mode:** transmission, diffuse reflectance infrared Fourier-transform (DRIFT), ATR; combination with heat cell, microscopy, sample preparation in transmission and ATR can induce polymorphic transformations **Burger´s infrared rule (attempt to predict stability):** for polymorphs dominated by hydrogen bonding the polymorph with the first absorption band at higher frequency will have higher entropy, thus be less stable.
NIR Spectroscopy (Ph.Eur. 2008d)	**True polymorphs & solvates:** band shift and splitting – change of molecular symmetry **Isomorphic desolvates:** loss of solvent peaks, shift of drug peaks, hydrogen bonding interaction **Amorphous solids:** peak broadening, lack of low frequency vibrations, molecular mobility	**Spectra:** overtone and combinations of FT-IR spectral bands, dipole moment change, scattering differences	**Mode:** transmission, diffuse reflectance, transflectance; sensitivity to water; **multivariate data analysis:** separation of physical from chemical information.
Raman Spectroscopy (Ph.Eur. 2008e)	**Isomorphic desolvates:** loss of solvent peaks, shift of drug peaks **Amorphous solids:** peak broadening	**Spectra:** change in polarisability, Stokes scatter presented as Raman shift cm^{-1}	**Mode:** backscatter, transmission, combination with microscopy; complementary information to IR, no sample preparation, not water sensitive, fluorescence (also of excipients) interferes, local sample heating (Johansson et al. 2002)

2.2.1. Hydrate formation

The formation of hydrates, a subclass of solvates, has been reported for a significant number of the APIs (Bechtloff et al. 2001). Hydrates usually exhibit different crystal packing, thus showing changes in intermolecular interactions and crystalline order. These changes influence solubility, dissolution rate, stability, and bioavailability (Khankari & Grant 1995). The nearly ubiquitous presence of water in various pharmaceutical manufacturing steps underlines the importance of monitoring hydrate formation during critical processing steps (e.g. wet granulation, aqueous film-coating).

Hydrates can be classified into isolated site hydrates, channel hydrates, and ion associated hydrates (Morris 1999) depending on the location of the water molecules in the crystal structure of the API. In isolated site hydrates water molecules are located in a manner such that they are not in direct contact. Channel hydrates provide channels or planes to accommodate the water molecules, which are usually located next to each other. Channel hydrates release the water molecules more readily than isolated site hydrates and can result in isomorphic, dehydrated structures. In this situation the crystal structure of the channel hydrate merely relaxes upon dehydration, creating a hygroscopic anhydrous form (Stephenson et al. 1998). The process is reversible; in high humidity the crystal lattice expands to take up water molecules (Datta & Grant 2004). In the last category, the ion associated hydrates, water molecules are coordinated by ions that are incorporated in the crystal lattice.

The effects of relative humidity and water activity are important when determining whether the hydrate or the anhydrous form of an API is stable under the applied conditions (Li et al. 2008). Since the anhydrate has a higher free energy, the bioavailability is usually higher than for the corresponding hydrate. Therefore, anhydrous forms are often favoured for manufacturing. A study revealed that the thermodynamically more stable anhydrate of carbamazepine (form III) had a lower intrinsic solubility than the thermodynamically less stable anhydrate (form I) but a higher bioavailability. The thermodynamically less stable anhydrate and the dihydrate showed comparable results concerning the bioavailability, which is a result of the fast transformation of form I into the dihydrate form in solution (Kobayashi et al. 2000). Transformations of azithromycin anhydrate, dihydrate, and monohydrate were studied in accelerated storage conditions using NIR spectroscopy to assess the stability (Blanco et al. 2005). NIR spectroscopy was used to identify the most stable form as the dihydrate, which supported the findings of Gandhi et al. (2002). NIR and Raman spectroscopy were used to monitor theophylline and caffeine hydrate formation during wet granulation (Jørgensen et al. 2002).

2.2.2. Dehydration

The mechanism of dehydration of organic solids has been studied extensively. The topic is highly relevant for pharmaceutical research because in nearly every

production cycle of pharmaceutics the intermediate or final product will be exposed to a drying step of some sort. The formation of different polymorphs (Petit et al. 2007), amorphous material, or hygroscopic dehydrated forms (Stephenson et al. 1998) may result in further solid-state transformations during storage, which in their turn may result in different stability and bioavailability.

With the aim to model dehydration behaviour Petit and Coquerel (1996) have proposed a dehydration theory based on their investigation of dehydrate and anhydrous copper (II) 8-hydroxyquinolinate. Depending on certain criteria the removal of water can be classified as destructive or cooperative (Figure 1). In essence, this can be explained as follows: if sufficiently large planes or channels exist in the molecular structure of a hydrate *(I)*, water will be released cooperatively accompanied by a decrease of molecular volume of the crystal and an overall decrease in the identical structural order *(I*)*. If the water release does not induce significant deformation in the crystal, the resulting form will be isomorphic *(I')* to the hydrate structure and will have a high probability of converting back into the hydrate form at higher relative humidity. This process belongs to the class II topotactic mechanism. If the release of water does not appear smoothly, but results in domains with cracks and defects, the crystal will reorganise (class II *coop*erative-*reorg*anisation) but retain structures of the hydrate form *(I_a).* If these domains are small and sufficiently numerous, the surface energy will be too high for reorganisation and either the system will crystallise via a nucleation growth process (class I *coop*erative-*cryst*allisation) and form a new crystal structure *(II)* or result in amorphous material (class I *coop*erative-*disorg*anisation). If the planes or channels, however, are not large enough or the liberation energy of the water molecules is too high, the process will result in destruction of the crystal phase.

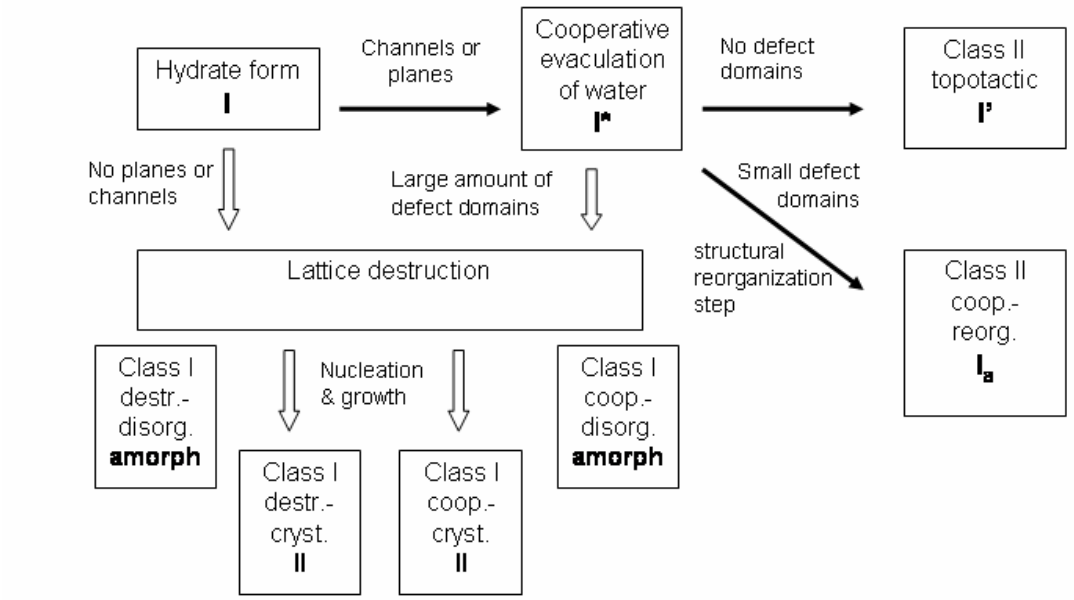

Figure 1. *Possible dehydration mechanisms for a hydrate (adopted from Petit & Coquerel 1996).*

In the class I *destr*uctive-*disorg*anisation mechanism no nucleation growth process occurs and the final material will be amorphous. The other possibility is the class I *destr*uctive-*cryst*allisation mechanism. In this case nucleation occurs and a new crystal *(II)* is formed. All prior structural information is consequently lost.

It should be noted that the kinetics of the dehydration process may lead to different mechanisms. Garnier et al. (2002) differentiate between smooth and hard dehydration conditions. For example, if water evaporates slowly, a certain material may follow the class II cooperative-reorganisation mechanism. Higher temperature and lower relative humidity can cause a class I cooperative mechanism for the same material. Nevertheless, heat and relative humidity are not the only parameters that significantly influence the dehydration kinetics. In order to investigate the dehydration process, one should also consider thermodynamic parameters, structural features of the hydrate, and physical factors (size, shape, defects) (Petit et al. 2007). Mechanical stress can also generate surface defects or induce local heating of the crystal due to, for example, milling and pressure during tabletting (Zhang et al. 2004).

Another classification scheme has been introduced by Galwey (2000) using the manner in which water evaporates as a criterion for the classification and the structural changes that occur after the loss of water to subdivide each class.

2.3. Vibrational spectroscopy

Since the PAT initiative of the FDA at the beginning of this decade, vibrational spectroscopy has steadily gained importance in pharmaceutical research and industry. This initiative resulted in the general conclusion that “quality cannot be tested into products; it should be built in or should be by design” (FDA 2004a). Vibrational spectroscopy offers a lot of advantages for PAT applications ranging from fast data acquisition with non-destructive and non-invasive measurements to minimal or no need for sample preparation. The techniques provide different information about the molecular state and its changes. Raman spectroscopy probes the change in polarisability while infrared spectroscopy measures a change of dipole moment in a molecule. Available methods should therefore be used in complement with each other in order to obtain a more complete picture of the molecular structure of the compound (Giron et al. 2002). A combination of the spectroscopic methods has been particularly beneficial for polymorph screening (Aaltonen et al. 2007a). In addition, other methods like XRPD and microscopic methods should be also taken into consideration for investigating polymorphism (Yu et al. 1998).

Absorption of electromagnetic radiation occurs when the energy of the radiation correlates with the energy of molecular vibration within a molecule. The forms of energy that contribute to the absorption in the infrared region are vibrational energy (component atoms vibrate around the mean centre of their chemical bond) and rotational energy (tumbling motion). The infrared region can be divided into near- (12800 – 4000 cm^{-1}), mid- (4000 – 400 cm^{-1}), and far-infrared (400 – 10 cm^{-1}) regions. The far-infrared region includes the region that is known as the terahertz

gap. Rotational energy of the molecules mainly accounts for absorption in the far-infrared region. Molecular vibrations can be classified into stretching, if the distance between the atoms changes and bending, if the bond angle changes. In general bending vibrations occur at lower frequencies than the corresponding stretching vibrations (Coates 2000). Also the bond strength and the mass of the atoms can be correlated to the frequencies at which the molecule absorbs: the stronger the bond (single, double, triple bond) the higher the frequency and the greater the mass of the atoms the lower the frequency.

In the mid-infrared region largely fundamental vibrations occur, which correspond to the excitation from the ground electronic state (ν_0) to the first excited vibrational energy state (ν_1). NIR region corresponds to overtones (ν_2, ν_3, …) and combinations of the fundamental vibrations, mainly of CH and OH stretch combination bands and CH, OH and NH overtones (Figure 2a).

A molecule is infrared active if the dipole changes upon vibration. The larger the dipole change the stronger the intensity of the absorption band. For being Raman active a molecule requires a change in polarisability (inducing a dipole) during the vibration or rotation. This dipole emits or scatters light at the optical frequency of the incident light wave. Often infrared active molecules with a dipole are not Raman active and vice versa. The two techniques should be considered as complimentary, as can be seen in Figure 2b showing fundamental stretching (ν) and deformation (δ) vibrations occurring in Raman and infrared spectroscopy.

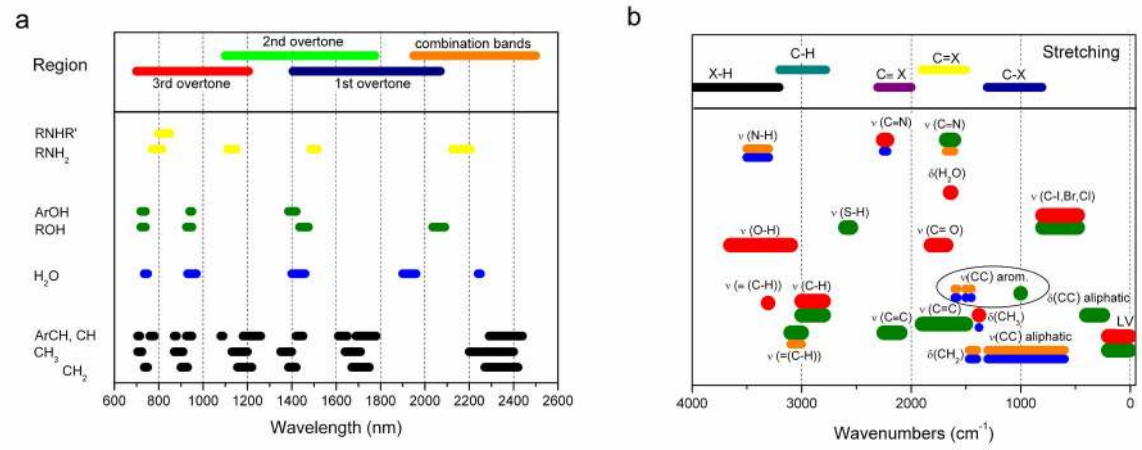

Figure 2. *Characteristic overtone and combination vibrations in the near-infrared region (a). Absorbance bands and lattice vibrations (LV) in Raman (green: strong signal, blue: medium signal) and infrared (red: strong signal, orange: medium signal) spectroscopy (b), X = N, O, C and S (modified from Coates 2000, McCreery 2000, Workman 2000).*

For quantitative analysis in Raman spectroscopy the intensity of the signal is directly related to the concentration of the compound (Siesler 2002). In the case of ultraviolet/visible, mid-infrared, near-infrared, and far-infrared spectroscopy the Beer Lambert law (Eq. 1) can be used as a reasonable approximation for the concentration of a component in a system. It describes the linear relationship

between the absorbance (*A*) and the molar concentration (*c*) using the molar absorptivity (α) and the optical pathlength (*d*).

(1) $$A = \alpha\, d\, c = \log\left(\frac{I_0}{I}\right)$$

Due to the complexity of most systems measured the Beer Lambert law has to be modified to account for interference by other components in the system and for different morphologies, which result in different interaction of the radiation with the sample. Nevertheless, using the Beer Lambert law one can develop calibrations relating spectral signal to sample concentration (Heise & Winzen 2002).

2.3.1. Near-infrared spectroscopy

The probability of transitions to higher excited states ($>\nu_1$) is considerably lower compared to transitions to the first excited vibrational energy state (ν_1), which leads to one of the major advantages of NIR spectroscopy: while the sample has to be diluted for analysis using mid-infrared spectroscopy due to the high level of absorption, NIR spectroscopy can recorded spectra without any sample preparation. The molar absorptivity in the NIR region is usually 10 – 100 times weaker compared to the absorptivity of the corresponding fundamental bands in the mid-infrared region (Reich 2005). The lower molar absorptivity and the lower frequencies used in the NIR region result in another advantage: NIR radiation has a greater penetration depth compared to mid-infrared radiation.

One of the disadvantages of NIR spectroscopy is the broad overlapping bands in the spectra, which makes interpretation more difficult (Reich 2005). This leads to restricted sensitivity and poor resolution. The interfering physical information, resulting in baseline effects and the need to extract chemical information from these complex spectra, calls for multivariate data analysis (Heise & Winzen 2002).

For in-line applications NIR measurements are performed in combination with a diffuse reflectance probe attached by fibre optics to the spectrometer. An incident beam hits the surface of the sample with one part of the beam being reflected, with a specular and a diffuse component, and the other part being transmitted. The diffusely reflected light accounts for most of the spectral information obtained by NIR reflectance spectroscopy and can be divided into refracted, randomly reflected, and scattered components. The reflected light contains chemical information leading to the identification of materials or quantification of the absorbent concentration (Blanco et al. 1999) using the Beer Lambert law (Eq. 1). In a similar manner the coating thickness can be determined (Kirsch & Drennen 1995, 1996).

Physical properties of the sample affect the reflected light and interfere with the chemical information of the spectra. This can also be used to determine particle size changes (Ciurczak et al. 1986, O'Neil et al. 1999, Otsuka 2004, Rantanen & Yliruusi 1998, Rantanen et al. 2005) during a process. The decrease in scattering due to an increase of particle size leads to deeper penetration of the light and thus to an increase of apparent absorbance. Another parameter that can be assessed is the

density of the sample, which has been used to predict the crushing strength of tablets (Kirsch & Drennen 1995), the density of compacts produced by roller compaction (Gupta et al. 2005), and the rheological properties of a granulated mass (Jørgensen et al. 2004).

Despite the dependence on multivariate data analysis for extracting information from NIR spectral data, numerous applications for NIR spectroscopy have been found in pharmaceutical research and industry: the identification of raw materials for example different grades of pharmaceutical excipients (Yoon et al. 1998) or counterfeit drugs (Scafi & Pasquini 2001), monitoring the blend uniformity on-line (Hailey et al. 1996), and measurement of coating thickness (Andersson et al. 1999, 2000, Pérez-Ramos et al. 2005). In addition, critical parameters during drying for low-melting APIs (Wildfong et al. 2002) and the drug content in mucoadhesive thin-film composites have been investigated (Fountain et al. 2003).

Moisture content analysis is another broad application in many industries including pharmaceuticals (Berntsson et al. 1997, Rantanen et al. 1998, 2000), since water is a strong absorber in the NIR region. NIR spectroscopy is very sensitive to the presence of water molecules (Stein & Amrose 1963) and hydrogen bonds (Maeda et al. 1995). The combination band of water is located at 1940 nm and the first overtone vibration can be found at 1450 nm. Depending on the interactions of water with solids these bands can shift, enabling the distinction between hydrate bound water and liquid water (Buckton et al. 1998, Jørgensen et al. 2002). Furthermore, NIR spectroscopy was able to detect polymorphic forms (Yu et al. 1998) and hydrate formation (Crucio and Petty 1951, Jørgensen et al. 2002, Kogermann et al. 2007, Aaltonen et al. 2007b).

Calibration models for NIR measurements, for example, to quantify the content of API in a tablet can be time consuming to prepare. Blanco et al. (2000, 2008) have therefore investigated the possibility of reducing the time and work load for these calibration models. They produced laboratory samples with sufficient variability (Blanco et al. 2008) to prepare a single PLS regression model that assessed the API content in the blend and the final tablets. This model was then used to predict the API content of production samples. The extent of polymorphic transformation during granulation was modelled separately using multivariate curve resolution – alternating least squares; a method that can provide spectral and concentration profiles for an evolving process (de Juan & Tauler 2003, 2006). Recently, Abrahamsson et al. (2005) measured the API content of intact tablets using time-resolved transmission NIR spectroscopy, which is less sensitive towards the physical properties of tablets.

For further information about NIR spectroscopy in the pharmaceutical field the reader is referred to the review articles, which have been published by Luypaert et al. (2007), Räsänen & Sandler (2006), and Reich (2005). Interesting reviews from other scientific fields have been published by Huang et al. 2008, who has discussed use of NIR spectroscopy in the food and beverage industry, and Workman (1999), who has published an extensive review about NIR and infrared spectroscopy. He gives examples for applications and different measurement methods in a variety of fields.

2.3.2. Terahertz pulsed spectroscopy and imaging

Terahertz spectroscopy has been under development for years before more efficient power sources (ultra-short pulsed lasers) and more sensitive detectors (semiconductor receivers) made it available for broader use. Applications for terahertz spectroscopy have been tested, for example, in the medical field of cancer detection (Woodward et al. 2003), and imaging of teeth (Crawley et al. 2003), as well as for material characterisation. Ferguson and Zhang (2002) have published a detailed review on different terahertz spectroscopic systems and their current applications. The discussion includes advantages and disadvantages of the available terahertz sources (using either photoconduction or optical rectification) and terahertz detectors. In the past highly sensitive terahertz detectors (e.g. helium cooled silicon bolometer) were required that were cryogenically cooled to reduce the interference of the thermal background. The commercially available set-up (TPS 2000^{TM}, TeraView Ltd, Cambridge, UK) uses NIR laser pulses at 80 MHz, which are focussed onto a GaAs photoconductive switch acting as the terahertz emitter. The laser beam generates electron-hole pairs, which are accelerated in an electric field and consequently emit pulsed terahertz radiation. An optically gated semiconductor receiver antenna (similar to the terahertz emitter) is used for detection of the terahertz signal that passes through the sample. A small part of the incident NIR laser pulse is directed via an optical delay-line onto the semiconductor receiver, generating electron-hole pairs. The resulting electric field induces a reference photocurrent that can be used for measurement at the receiver. Time gating allows detecting the amplitude and phase of the terahertz pulse and provides information about the absorption coefficient and, provided the thickness of the sample is known, its refractive index (Taday & Newnham 2004).

Terahertz radiation (3 - 333cm^{-1} or 100 GHz - 0 THz) is a part of the far-infrared region, which is located between the infrared and the microwaves region of the electromagnetic spectrum. One of the major advantages of the low energy terahertz radiation is the reduced probability of sample degradation. Hydrogen bond vibrations (Jakobsen et al. 1968) and low energy lattice vibrations, so called crystalline phonon vibrations (Taday & Newnham 2004), absorb in the terahertz region. These are important vibrations of solid materials because they are directly affected by changes in crystal structure, such as polymorphic transformations. Comparable to XRPD there is little information obtained from amorphous materials in the terahertz region. The lack of the long-range order prevents propagation of the vibration and the energy expands diffusely within the material or scatters (Zeitler et al. 2007b). Since most of the pharmaceutical excipients that serve as tablet or capsule fillers are amorphous or partly amorphous, they are often transparent or semitransparent to terahertz radiation. Thus, they cause no or little interference when investigating crystalline drugs. Recently, amorphous material was characterised using TPS while heating the sample. Structural relaxation and increase in molecular mobility for the amorphous sample were visible in the absorbance spectra when transforming to the glassy or rubbery state (Zeitler et al. 2007c).

In addition to the intermolecular vibrations, the terahertz spectral information may contain low frequency intramolecular vibration making it complicated to assign bands (Taday 2004). Nevertheless, initial attempts to reveal the origin of the bands in the phonon spectra of carbamazepine have shown promising results (Day et al. 2006). The authors compared spectra calculated from harmonic rigid molecule dynamics calculations on the polymorphic structures using boundary conditions to the spectra of the polymorphic forms, taken at low temperature. Promising results in assigning bands were also achieved by comparing solid-state density functional theory calculations to the terahertz spectra of an explosive (Allis & Korter 2006).

TPS has been successfully used to determine polymorphic forms of various APIs. Kogermann et al. (2007) have shown that dehydration of piroxicam was detectable in compacts. Strachan et al. (2004) have investigated polymorphic forms of carbamazepine, enalapril maleate, indomethacin, and fenoprofen calcium. In a subsequent study by the same authors (Strachan et al. 2005) TPS was used to quantify the degree of crystallinity and polymorphism in binary mixtures in conjunction with partial least squares (PLS) regression. Furthermore, the content of acetaminophen in tablets was measured in transmission mode and results were compared to the destructive standard method, high performance liquid chromatography (HPLC) (Spencer et al. 2007). In order to characterise powders, formulated products, and liquids, terahertz spectra can also be obtained with an attenuated total reflection (ATR) module requiring minimal or no sample preparation (Gradinarsky et al. 2006, Newnham & Taday 2008).

Another application in the pharmaceutical field is the imaging of solid dosage forms, e.g. coated tablets, and soft and hard gelatine capsules (Fitzgerald et al. 2005, Zeitler et al. 2007a). A change in the physico-chemical properties at a sample interface is visible in the terahertz time domain waveform. This is due to a change in the refractive index (RI) and absorption coefficient in the sample material. TPI derives coating quality related information from the surface and interface reflection of the sample. The technique has been employed to determine the coating thickness of single and multiple layer-tablets, coating uniformity, and coating integrity in a non-destructive manner using the time domain information and the terahertz electric field peak strength (TEFPS) (Zeitler et al. 2007a, b, Ho et al. 2008). The TEFPS can be calculated from the signal reflected off the coating surface normalised by the magnitude of the incident pulse: though it is sensitive to scattering effects, it can be used to gain information on the density of the coating. Using the information of the scattering effects the TEFPS can be used to detect surface roughness. Furthermore, it was possible to relate the differences in TEFPS to the dissolution behaviour of sustained-release coated tablets and to changes in the process parameters during the coating operation (Ho et al. 2008). Depending on the system that is analysed and the frequency that is used, the penetration depths lies between 1 and 3 mm (Zeitler et al. 2007a) with a depth resolution of 40 µm, a spectral resolution of 1 cm^{-1}, and a spatial resolution of 50 µm. A detailed description of the TPI device can be found in the work of Zeitler et al. (2007a, b). Comprehensive reviews about analysis of solid dosage forms with terahertz spectroscopy in general have also been recently published (Strachan et al. 2006, Zeitler et al. 2007b).

2.3.3. Raman spectroscopy

When a molecule absorbs energy, in this case monochromatic light from a laser source, it may enter a higher virtual energy state. The molecule can then relax back to the ground electronic state by emitting the same amount of energy that was taken up resulting in elastic scattering (Rayleigh scattering). In addition, a small part returns to a different energy level than the incident one, so called inelastic scattering. Depending on the incident energy state of the molecule this inelastic scattering can lead to a higher energy state of the molecule (Stokes shift) or to a lower energy state (anti-Stokes shift). Usually in Raman spectroscopy Stokes shifts are reported because they have a greater intensity. The disadvantage of detecting Stokes scattering is that, depending on the structure of the molecule, fluorescence can obscure the Stokes signals. Anti-Stokes shifts do not suffer from this interference; but require molecules to be in a vibrational excited state; a situation that is negligible at room temperature.

As Raman spectroscopy is readily applicable in-line and offers the possibility for obtaining real-time data, it has been frequently used to gain insight into pharmaceutical unit operations on a molecular level (Rantanen 2007). Water is a poor Raman scatterer, thus Raman spectroscopy is an ideal method for monitoring processes in which water signals may overwhelm spectra obtained with other spectroscopic methods. It can be used to detect hydrate formation (Airaksinen et al. 2003, Jørgensen et al. 2002, Wikström et al. 2005), determining the conversion kinetics between polymorphic forms in aqueous environment (Tian et al. 2006), assessing the interaction of water with polymers (Taylor et al. 2001), and detecting solid-state changes during fluid-bed drying (Aaltonen et al. 2007b, Hausman et al. 2005). Recently, trace crystallinity of amorphous APIs has been investigated after milling (Heinz et al. 2008) and after compression of a model tablet formulation to a compact (Okumura & Otsuka 2005). The application of Raman spectroscopy has expanded to characterising PITs of an API in final tablets (Taylor & Langkilde 2000) and quantifying API content in tablets (Johansson et al. 2005). Bulk solid dosage forms have been examined in transmission mode (Matousek & Parker 2006, Johansson et al. 2007), which was found to be more suitable for quantitative analysis than reflection mode due to the larger sampling volume. The coating variability was also investigated with Raman spectroscopy (Romero-Torres et al. 2005) as well as coating thickness (Romero-Torres et al. 2006, Kauffman et al. 2006). Raman spectroscopy was found to be an effective method for detecting counterfeit pharmaceutical products (Fernandez et al. 2008).

2.4. Data analysis

With the increasing amount of spectral data obtained by in-line monitoring of entire processes with vibrational spectroscopy chemometrics have become an important tool for PAT applications in pharmaceutics. The FDA has included chemometrics, being “multivariate tools for design, data acquisition and analysis”, as one of the PAT

tools in their PAT initiative (FDA 2004a). Chemometrics have been successfully applied in combination with vibrational spectroscopy in, for example, polymer chemistry (Lachenal 1994) or agricultural and food science (Foley et al. 1998).

Lavine and Workman (2006) have recently published a review in which they defined chemometrics being a “data microscope”. The use of multivariate data analysis may enable detection of a cause-and-effect relationship between variables, thus relating the association of variables with physical, chemical or biological phenomena. It may also mislead the analyser and therefore should be applied carefully. Data pre-treatment is a science in itself and the quality of the achieved model depends greatly on the methods used to initially remove unwanted data variation. To avoid pitfalls it is important to understand the source of the variation within the data set (Doherty & Lange 2006), which can also be a result of an instrumental problem or external interference. Another key ingredient to achieve a reliable model is to use a representative test and training set (Brereton 2005). The use of multivariate data analysis includes explorative data analysis, multivariate regression and pattern recognition (classification).

2.4.1. Data pre-treatment

The methods of data pre-treatment can be divided into two groups. The first are row-wise methods, which remove unwanted variance from each sample spectrum at a time and should be applied first. The second group are the column-wise methods, which act on the variables of the data and include all variance for their calculation. Mean centering (MC), for example, is a column-wise method and centres the data relative to the mean of the data set. This emphasises the differences in the spectral features of the dataset. The simplest pre-treatment of the data is to select a certain wavelength range that contains mainly noise and/or unimportant information and exclude this range from the data set.

2.4.1.1. Savitzky-Golay smoothing and derivatives

Savitzky-Golay smoothing on its own is a powerful method to remove spectral noise. For optimising the smoothing process it is possible to select the filter width and the polynomial order (Savitzky & Golay 1964). Since the selection is dependent on the application e.g. for Raman spectra containing sharper peaks than NIR spectra, a smaller filter width should be selected.

Derivatives in combination with Savitzky-Golay smoothing remove baseline offsets and additionally scale the data depending on their frequency. This means for a first derivative operation the low frequency signals decrease in their signal strength while the higher frequency signals gain more importance. This also holds true for the second derivative. But it should also be mentioned that noise is a high frequency signal and will be emphasised as well. The signal-to-noise (S/N) ratio therefore decreases, as a result of the increase in noise and the decrease in actual signal

compared to the initial absorbance. For detailed information about the behaviour of derivatives and computational limitations in estimating true derivatives of real data the reader is referred to the work of Mark & Workman (2003a, 2003b, 2003c, and 2004). The authors conclude that calculating derivatives may easily result in a decreased S/N ratio. Therefore, it is important to choose the setting for the convolution function carefully and on a case-by-case basis. When performing the smoothing operation, it is important to determine the best parameters for convolution, optimum spacing, and polynomial. Combined with the "right"-order derivative this may result in an improved S/N ratio.

2.4.1.2. Standard normal variate correction

Standard normal variate (SNV) correction normalises the data. Scaling and offset effects, so called multiplicative effects, are removed by this operation. SNV correction centres each spectrum around zero intensity by subtracting the average of all the spectral responses in the vector from each of the original values. In addition, each spectrum is divided by its standard variation (Barnes et al. 1989).

2.4.2. Principal component analysis

Principal component analysis (PCA) is used to compress the data set by explaining variance using principal components (PCs). It describes major trends within a dataset by capturing the maximum variance.

X is the matrix of independent variables (eg. spectral intensities) and contains N samples (columns) and M variables (rows). *X* will be decomposed into the scores matrix *T* (an N-by-A matrix), with the number of PCs being A, the loadings matrix being *P* (an M-by-A matrix), and the matrix *E* (N-by-M) containing the residuals.

(3) $$X = TP' + E$$

The first PC describes the greatest amount of variance in the data set. It passes through the origin and describes the maximum variance of the data. The second PC is orthogonal (independent) to the first PC and describes the second most variance. With every subsequent PC the variance decreases. Consequently, after a certain amount of variance explained the subsequent PCs will only contain noise. It is therefore important to select the optimal number of PCs to include only meaningful data in the model. There are several methods to detect the optimal number of PCs. One is to plot the number of PCs against the eigenvalues, which result from the decomposition of the original matrix. If the ratio of the eigenvalues for the two successive PCs drops drastically, starting from the first PC, the following PCs should not be included in the model.

In order to interpret the PCA model, the lack of fit Q (squared process error) helps to describe the influence of a sample on the model and can be used to detect

outliers. The Hotelling T^2 describes the leverage of a variable or the variation in each sample within the model. It can be presented as a geometrical distance to the mean of the data and thus outliers can be detected visually.

PCA is a popular data analysis method in pharmaceutical research. It has been used to detect hydrate formation (Jørgensen et al. 2002) and different phases during fluid-bed granulation (Rantanen et al. 2005). Tablets compressed with either a single punch or rotary tablet press were classified with PCA according to their tablet hardness (Cogdill et al. 2005a).

2.4.3. Partial least squares regression

Partial least squares (PLS) regression (Wold 1966, Wold et al. 1983, Wold et al. 2001) combines features of PCA and multiple linear regression in order to create a model between X and Y scores. It is an iterative method, which is used to develop a linear model. This model combines fundamental relationships between the measured variables, X, and a property of interest, Y (unlike PCA, which does not use Y in the calculations). So the first step of a PLS regression is a decomposition step, comparable to PCA, and the detection of components, here called latent variables (LVs). These components should explain the covariance between X and Y. This is followed by a regression step to achieve correlation.

As in PCA, the selection of a suitable number of latent variables is important; otherwise the model may be overfitted or underfitted. One of the methods that is frequently used in chemometrics applies cross-validation. During cross-validation samples of the data set are grouped into subsets. The performance of the model achieved using one of these subsets can be tested with unseen data (remaining subsets) and results in the root mean squared error of cross-validation (RMSECV). In the predicted error sum of squares (PRESS) plot the number of latent variables is then plotted against the RMSECV. The increase after a minimum in the RMSECV indicates overfitting. Another sign of overfitting is the presence of noise-related features in the regression vector, which tries to combine a good fit to the observed variables with the ability to accurately predict variables. If noise is included in the model and correlates with X, it will be reflected in the regression vector and will lead to poor predictions.

PLS regression of multivariate data has been employed to quantify polymorphic and pseudo-polymorphic transformations, for example, during storage (Blanco et al. 2005), to predict the API content in compressed tablets (Cogdill et al. 2005b), and to determine the coating thickness (Andersson et al. 2000). Chalus et al. (2007) compared modelling the drug content in tablets using PLS regression and artificial neuronal network. In this study the artificial neuronal network model provided greater linearity and correlation between the reference and the predictions than the PLS model.

3. Aims of the study

In order to gain a better insight into pharmaceutical manufacturing processes, PAT was applied to a variety of processes, such as blending, wetting, drying, and coating. These processes were investigated by vibrational spectroscopy. Specific aims of this study were:

- to obtain the optimal blending time for a double cone mixer by monitoring the blending process at-line with NIR spectroscopy
- to investigate the solid-state changes of APIs during granulation, extrusion, and spheronisation with Raman and NIR spectroscopy using XRPD as a reference method,
- to study the solid-state changes of an API during drying processes by first testing the suitability of the Raman and NIR spectroscopy at-line during an oven-bed drying process and then applying NIR spectroscopy in-line into a fluid-bed drying process,
- to investigate the potential of a novel small-scale coating device to obtain a calibration model for coating thickness prediction that can be applied to a coating drum process using NIR spectroscopy,
- to test the potential of TPI as an off-line analytical tool for coating quality assurance.

4. Experimental

Details about the experimental materials and methods are reported in the original publication (I-V) and are summarised below.

4.1. Materials

4.1.1. Raw materials

The model compounds used in publication I were anhydrous theophylline (100 M, Ph Eur, Orion Pharma, Espoo, Finland) and anhydrous nitrofurantoin (Sigma-Aldrich Chemie, Steinheim, Germany). For preparing pellets in publication I lactose monohydrate (80 M, Pharmatose; DMV Pharma, Veghel, The Netherlands) and microcrystalline cellulose (50 M, Emcocel; Penwest Pharmaceuticals, Nastola, Finland) were used.

Erythromycin dihydrate (Pharmacia&Upjohn Company, Kalamazoo, MI, US) was used in publications II and III with microcrystalline cellulose as a filler (Avicel® PH101, FMC, Cork, Ireland) for the pellets.

For publication IV the tablets contained high density polyethylene (PE, Inducted, Volketwil, Switzerland, particle size <10 µm) and amorphous fumed silica (Aerosil® 200, Degussa, Essen, Germany). The coating solution consisted of a polyvinyl acetate (PVA) suspension (Kollicoat SR30D®, BASF, Ludwigshafen, Germany) and a polyvinyl alcohol-polyethylene glycol graft copolymer (Kollicoat IR®, BASF, Ludwigshafen, Germany), triethylcitrate (Fluka, Buchs, Switzerland), glycerol monostearate (BDH Chemicals Ltd., V W R International, Poole, England), and polysorbate 80 (Tween® 80 V Pharma, Uniqema, Everberg, Belgium). The solvent used in all studies was purified water.

The tablets compressed for publication V contained diprophylline (BASF, Ludwigshafen, Germany), lactose monohydrate (Flowlac®, Meggle Wasserburg GmbH, Wasserburg, Germany), and vinylpyrrolidone-vinyl acetate copolymer (Kollidon VA 64®, BASF, Ludwigshafen, Germany). The sub-coat composition contained Kollicoat VA 64 and polyethylene glycol (PEG) 600 and for the main coat composition Kollicoat SR30D®, Kollicoat IR®, talc, FD&C blue dye (BASF, Ludwigshafen, Germany), and triethylcitrate were used.

4.1.2. Preparation of pellets (I-III)

The powders were dry-mixed in a double cone mixer. Pellets were manufactured using continuous extrusion-spheronisation (Nica M6L mixer/granulator; Nica E140 radial screen extruder; Nica S320 spheroniser; Nica System AB, Sweden). The blended powder mixture was wetted with purified water in a mixer/granulator.

4.1.3. Preparation of tablets cores (IV)

The composition, containing HDPE and Aerosil® 200, was mixed with a Turbula® mixer (Bachofen AG Maschinenfabrik, Basel, Switzerland). Flat-faced tablets and biconvex tablets (punch diameter = 9 mm) were compressed using an instrumented single punch tablet machine (Korsch EK0, Erweka Apparatebau, Berlin, Germany). The tablets (m = 170 mg) were compressed to a fixed load of 50 N.

4.1.4. Preparation of coating suspension (IV)

Purified water with polysorbate 80 was heated to 70°C and mixed with glycerol monostearate. The water soluble polymer Kollicoat IR® was dissolved in purified water. The achieved homogeneous solution was combined with Kollicoat® SR30D and the suspension containing polysorbate 80 and glycerol monostearate. Finally the plasticizer triethylcitrate was added. The whole suspension was stirred for 24 hours prior to use.

4.1.5. Preparation of sustained-release coated tablets (V)

The tablets were supplied by Bohle (L.B. BOHLE Maschinen & Verfahren GmBH, Ennigerloh, Germany). The sub-coat solution was prepared by dissolving Kollidon VA 64® in purified water and adding PEG 600. For the preparation of the coating suspension for the main coat Kollicoat IR® was dissolved in demineralised water and combined with the solution containing the dissolved colourant. Afterwards, firstly Kollicoat SR30D® and then the plasticizer, triethylcitrate, were added. The suspension was stirred for 24 hours and finally a suspension of talc in purified water was added.

4.2. Methods

4.2.1. Drying processes (II, III)

For publication II the pellets were dried in a conventional oven-tray dryer (Heraeus UT6760, Heraeus, Hanau, Germany) at 30°C or 60°C. Before sampling, the whole bed was circulated so that the sample was a representative mixture of pellets from all areas of the bed.

A multipart microscale fluid-bed powder processor (MMFD, Ariacon Oy, Turku, Finland) was used to dry the pellets (III) at 30°C, 45°C and 60°C. The moisture content of the inlet air was set to be 0.4 to 2.4 g water per kg of dry air at 22°C. The process was monitored by in-line NIR spectroscopy through the fluidisation chamber made of glass.

4.2.2. Coating processes (IV)

The flat-faced tablets, fitted into the moulds of the small-scale rotating plate device, passed a spraying unit, a heating unit (Sartorius thermo control, Sartorius AG, Goettingen, Germany), and an NIR probe during each rotation. A total of 20 tablets for each process were labelled, weighed, and their thickness was measured individually before and after the coating process using a digital micrometer (Sony digital micrometer U30-F, Sony Magnescale Inc, Tokyo, Japan).

The biconvex tablets were coated using an instrumented laboratory-scale side-vented drum coater (Thai coater, model 15, Pharmaceuticals and Medical Supply Ltd Partnership, Bangkok, Thailand) (Ruotsalainen et al. 2002). The coating batch comprised 1.0 kg tablet cores. Before and after coating 100 tablets were weighed and their heights were measured to calculate the coating thickness.

4.2.3. Near-infrared spectroscopy (I-IV)

For publication I and II the NIR measurements were made with a Fourier-transform (FT)-NIR spectrometer (Bomem MD-160 DX) using Bomem-GRAMS software (version 4.04; Galactic Industries Inc, Salem, NH, US) and Teflon as a reference (99% reflective Spectralon; Labsphere Inc, North Sutton, NH, US).

For papers III and IV the measurements were performed with a diffuse reflectance NIR spectrometer (NIR-256L-2.2T2, Control Development Inc., South Bend, IN, US) using a thermoelectrically cooled 256 array detector, a tungsten light source, and a fibre-optic reflectance probe, with Teflon serving as reference.

4.2.4. Raman spectroscopy (I)

The Raman spectra were measured at-line using a CCD Raman spectrometer (CDI Raman 785-1024; Control Development, Inc, South Bend, IN, US) with a 785-nm NIR diode laser (Starbright, Torsana Laser Technologies A/S, Skodberg, Denmark).

4.2.5. X-ray powder diffractometry (I-III)

X-ray powder diffraction (XRPD) was performed using a theta-theta diffractometer (D8 Advance, Bruker axs GmbH, Karlsruhe, Germany) operating in symmetrical reflection mode with CuK_{α} radiation (1.54 Å) and Göbel Mirror bent gradient multilayer optics. The scattered intensities were measured using a scintillation counter. Measurements were performed from 5 to 40º (2 theta) with steps of 0.05º (I) and 0.1º (II, III) and a measuring time of 1 s/step using a voltage of 40 kV and a current of 40 mA. Wet pellet samples of studies (II, III) were also measured with variable temperature XRPD.

4.2.6. Terahertz pulsed spectroscopy and imaging (V)

For studying the refractive index of the materials in the different coating solutions a TPS 1000^{TM} (TeraView Ltd, Cambridge, UK) was used. Each material was compressed with polyethylene into pellets. Samples were measured in transmission rapid-scanning mode and referenced against the spectrum of a pure polyethylene pellet for solids in dry nitrogen atmosphere.

The TPI^{TM} imaga 2000 system (TeraView Ltd, Cambridge, UK) was used to achieve 3D imaging of the sustained-release coated tablets. The data acquisition process consisted of two steps. A surface model was created at the laser gauge that formed the basis of the subsequent terahertz scan for construction of a 3D terahertz image. Terahertz mapping was performed in point-to-point scan mode with a step size of 200 µm. The axial resolution in the z-direction was about 38 µm. The data were analysed using the TPIviewTVL imaging software (version 2.3.0).

4.2.7. Moisture content analysis (I-III)

The moisture content of the pellets was analysed with a moisture content analyser (Sartorius moisture analyser MA 100 Sartorius GmbH, Göttingen, Germany).

4.2.8. Multivariate data analysis (I, III, IV)

For publication I the second derivative was calculated with MATLAB software (MATLAB 6.5; MathWorks Inc, Natick, Massachusetts, USA) using an 11-point, second order polynomial Savitzky-Golay smoothing operation. In publication III the data was pre-treated calculating a Savitzky-Golay first derivative with a filter width of 11-points and a second order polynomial fit. Furthermore, the data was SNV corrected and mean-centred. The data obtained for the coating processes (IV) was smoothed using a 21-point, second order polynomial Savitzky-Golay algorithm, then SNV corrected, and finally mean-centred.

The principal component analysis (PCA) for publication I was performed with SIMCA-P (SIMCA-P 8.0, Umetrics AB, Umeå, Sweden). The PCA analysis for publication III was performed with PLS-toolbox (PLS-toolbox 4.0.1, Eigenvector Research, Inc., Wenatchee, WA, US), as was the PLS regression model for publication IV.

5. Results and discussion

5.1. Solid-state properties

Theophylline (TP) belongs to the xanthine family of compounds. The therapy of respiratory diseases like asthma or chronic obstructive pulmonary disease (COPD) is its main therapeutic application. TP exists in two enantiotropic polymorphic forms: the anhydrate form I, which is stable at high temperatures, and the anhydrate form II, which is the stable form at room temperature (Burger & Ramberger 1979). Under conditions of high humidity or in aqueous environment the anhydrate forms readily convert to the monohydrate (Herman et al. 1988). Furthermore, there has been a metastable anhydrate identified (Phadnis & Suryanarayanan 1997).

Nitrofurantoin (NF) is an antibiotic used to treat urinary tract infections. There have been four polymorphic forms identified so far: NF monohydrate I and II and α and β anhydrate (Pienaar et al. 1993a, b). The β form of NF anhydrate has been used as the starting material in publication I and was readily identified by the NIR spectrum measured (Figure 3a, I). It showed characteristic peaks at 1551, 1631, 1701, 1745 and 1987 nm (Aaltonen et al. 2007b). NF monohydrate form II has been used as a reference was and has been found to be the more stable form (Otsuka & Matsuda 1994).

Erythromycin is a macrolide antibiotic. One of the different polymorphic forms of erythromycin (EM) is the channel hydrate EM dihydrate that tends to dehydrate upon drying. EM dehydrate is isomorphic to EM dihydrate (Stephenson et al. 1997, Miroshnyk et al. 2006) but highly hygroscopic (Stephenson et al. 1998), and thus prone to cause problems during processing (Bauer et al. 1999). The role of water as the solvent of crystallisation was found to be unique because desolvation of EM crystallised from other solvents (acetate, ethanol, isopropanol and methylethylketone) resulted in a collapse of the crystal lattice and formation of amorphous material (Mirza et al. 2003). EM can also exist as an amorphous form and an anhydrate. EM anhydrate recrystallises from the dehydrate melt at about 150°C (Stephenson et al. 1997, Miroshnyk et al. 2006). In this study EM anhydrate has not been considered for PITs due its high activation energy (Wang et al. 2006).

A scheme is presented in Table 3 summarising which techniques were used to gather information about a specific system during the unit operations.

5.2. Blending (I)

The blending of a three component formulation containing NF, microcrystalline cellulose (MCC), and lactose monohydrate was monitored by NIR spectroscopy. The data obtained during blending was analysed with PCA (first two PCs of the second derivative, Savitzky-Golay smoothed data). It was found that after 5 min the formulation was sufficiently mixed. After 10 min, there were no changes in

homogeneity detectable. Thus, NIR spectroscopy in combination with PCA was found to be a suitable process analytical tool to determine the optimal blending time.

Table 3. *Scheme of the processes monitored during the present work*

System	In-line	At/off-line	Technique used	Pharmaceutical unit operations	Information obtained
NF, TP, EM		X	XRPD, NIR and Raman spectroscopy	Raw materials	Identifying raw material, obtaining reference data for all known polymorphic forms
NF		X	NIR spectroscopy	Mixing	Blend uniformity, end-point detection
NF, TP, EM		X	XRPD, NIR and Raman spectroscopy	Granulation Extrusion Spheronisation	Hydrate formation for NF and TP, moisture content determination
NF, TP, EM	X	X	XRPD, Raman and NIR spectroscopy	Drying	Moisture content determination, following dehydration for NF, TP and EM, end-point detection
HDPE		X	NIR and Raman spectroscopy	Tableting	No changes after exposure to high pressure detectable
HDPE, coating solution	X	X	NIR spectroscopy, TPS and TPI	Tablet coating	Monitoring coating thickness development, characterisation of coating variations and uniformity

5.3. Extrusion-Spheronisation (I, II)

The manufacturing steps of pelletisation (granulation, extrusion and spheronisation) were analysed at-line using NIR spectroscopy, Raman spectroscopy, and XRPD. Due to the high water saturation of the samples, there was no chemical information that could be obtained by the NIR spectral data in any of the used formulations (I, II) containing either TP, NF (I), or EM (II). Nevertheless, the baseline shift indicated the increase of particle size after granulation, extrusion, and spheronisation (Figures 2 and 3, I).

With Raman spectroscopy it was possible to detect solid-state transformations of anhydrous TP and anhydrous NF upon wetting (I). The characteristic peaks between the anhydrous and the monohydrate form of TP were difficult to detect due to the low drug content (10% w/w) and were often obscured by excipient bands. Subtle changes in the area of 1700 to 1650cm^{-1}, however, indicated the formation of the monohydrate (Figure 5a, I). This finding was supported by the reflection pattern of the XRPD analysis, showing characteristic reflections at 11.4° (2θ) and 14.7° (2θ) for TP monohydrate after granulation (Figure 4b, I). Hydrate formation of anhydrous TP to the monohydrate form has been frequently reported (Jørgensen et al. 2002, Otsuka et al. 1990, Räsänen et al. 2001). Amado et al. (2007) have investigated hydrate formation of anhydrous TP, being a one step random nucleation process, with Raman spectroscopy and determined the critical relative humidity to be >79% at room temperature (Otsuka et al. 1990).

The formation of NF monohydrate was readily detectable by Raman spectroscopy (Figure 5 a and d, I) and confirmed by the change of XRPD reflections (Figure 4c, I). While the dry powder showed characteristic reflections for NF anhydrate at 14.4° (2θ) and 28.8° (2θ), the sample taken after granulation showed reflections at 13.9° (2θ) and 27.2° (2θ), which are characteristic for the monohydrate.

In the formulation containing EM dihydrate (II) it was not possible to detect any solid-state changes with Raman spectroscopy, even though the drug content was relatively high, at 50% w/w. Fluorescence, caused by the excipent MCC, obscured significant Raman bands. This made it impossible to differentiate between EM dihydrate, dehydrate, and amorphous EM. The XRPD reflection pattern, however, did not indicate any solid-state transformation during pelletisation (Figure 3, II). Considering that the formulation with EM contained a dihydrate and the forms that may occur required a dehydration process (dehydrate, anhydrate), or the loss of the long range order (amorphous EM) there were no solid-state changes expected during pelletisation.

5.4. Drying (I, II, III)

The effect of the drying temperature (60°C, 100°C and 135°C) for the pellets containing TP and NF (I) was investigated using an infrared drier. The Raman spectra and XRPD pattern of TP pellets dried at 60°C still contained characteristics of the monohydrate while the pellets dried at higher temperatures indicated dehydration to TP anhydrate (Figure 4b, I and Figure 5b, I). TP monohydrate is a channel hydrate and loses its water molecules readily at around 80°C (Aaltonen et al. 2007b). It forms the anhydrate via a metastable anhydrate form (Phadnis & Suryanarayanan 1997, Aaltonen et al. 2007b) with the dehydration process being reversible. Amado et al (2007) have detected structural similarities between TP monohydrate and the metastable anhydrate, which apparently retains the intermolecular interactions of the monohydrate. After this cooperative release of water molecules structural rearrangement is evident. This process is readily reversible and the average

crystallite size of theophylline monohydrate is higher than that of the anhydrate form (Airaksinen et al. 2004). Thus, it seems likely that the dehydration process of TP monohydrate follows the class II cooperative-reorganisation mechanism.

For the NF pellets the dehydration occurred only at the highest temperature of 135°C (Figure 4c, I and Figure 5c, I), but it was not possible to detect into which anhydrate NF transformed. Variable temperature XRPD analysis of NF monohydrate (Karjalainen et al. 2005, Kishi et al. 2002) detected formation of NF anhydrate at around 140°C via formation of amorphous material. In a high humidity atmosphere Kishi et al. (2002) were not able to detect any amorphous halo background when performing variable temperature XRPD. This indicates that at high humidity dehydration of NF monohydrate follows the Class I cooperative-crystallisation mechanism while at low humidity the Class I destructive-crystallisation mechanism is followed. The dehydration of NF monohydrate form II has been studied (Jørgensen et al. 2006) using differential scanning calorimetry with the onset of dehydration detected at 115°C. It gradually crystallises at temperatures between 132 and 137°C.

It is evident that TP loses its water molecules more readily than NF. This can be explained by the hydrate structure: NF is an isolated site hydrate while TP is a channel hydrate.

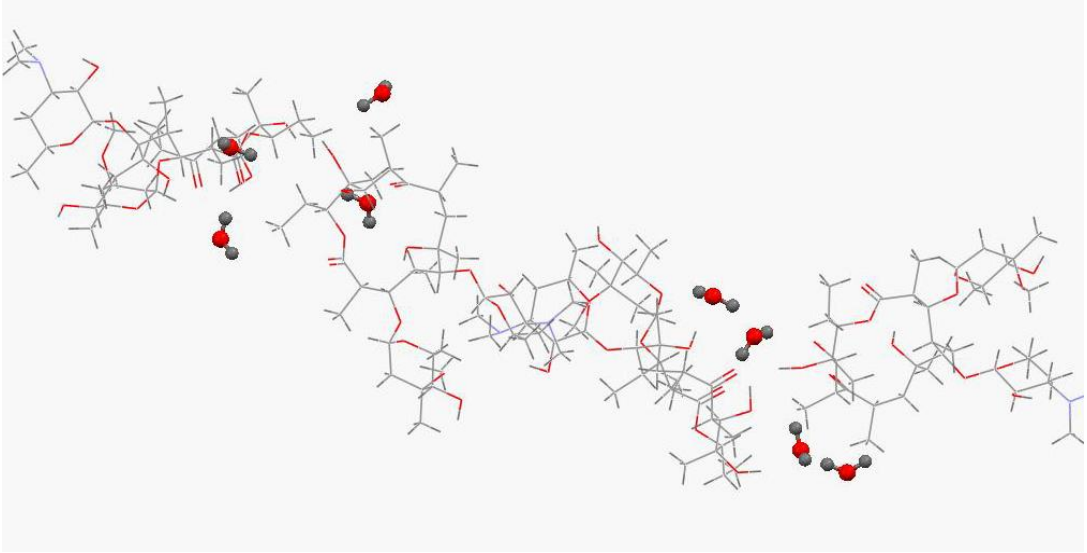

Figure 3. *Unit cell of EM dihydrate with the water molecules highlighted.*

For the study containing EM dihydrate (Figure 3) the crucial process step was the drying step. NIR and Raman spectroscopy were first tested at-line in an oven-bed drying process (30°C and 60°C). Solid-state changes were confirmed by XRPD. The oven-bed drying process had the advantage of providing easy access to the samples. The data obtained by NIR spectroscopy showed the occurrence of isomorphic EM dehydrate for one batch dried at 60°C (Figure 6c, II). Even though EM dihydrate and its dehydrated form have the same crystal structure, there are minor differences in the reflections of the XRPD pattern detectable. These distinct reflections occur at 9.9° (2θ), 10.3° (2θ) and 13.1° (2θ) for EM dihydrate and at 9.7° (2θ), 10.2° (2θ) and 13.3° (2θ), respectively, for EM dehydrate. The crystal lattice

merely relaxes when the water evaporates, causing these shifts in XRPD. Dehydration consequently follows the Class II topotactic mechanism (Miroshnyk et al. 2006).

The wet pellets (obtained after spheronisation) were additionally examined with variable temperature XRPD (Figure 7, II). At a temperature of about 70°C the reflection pattern was equivalent to that of EM dehydrate.

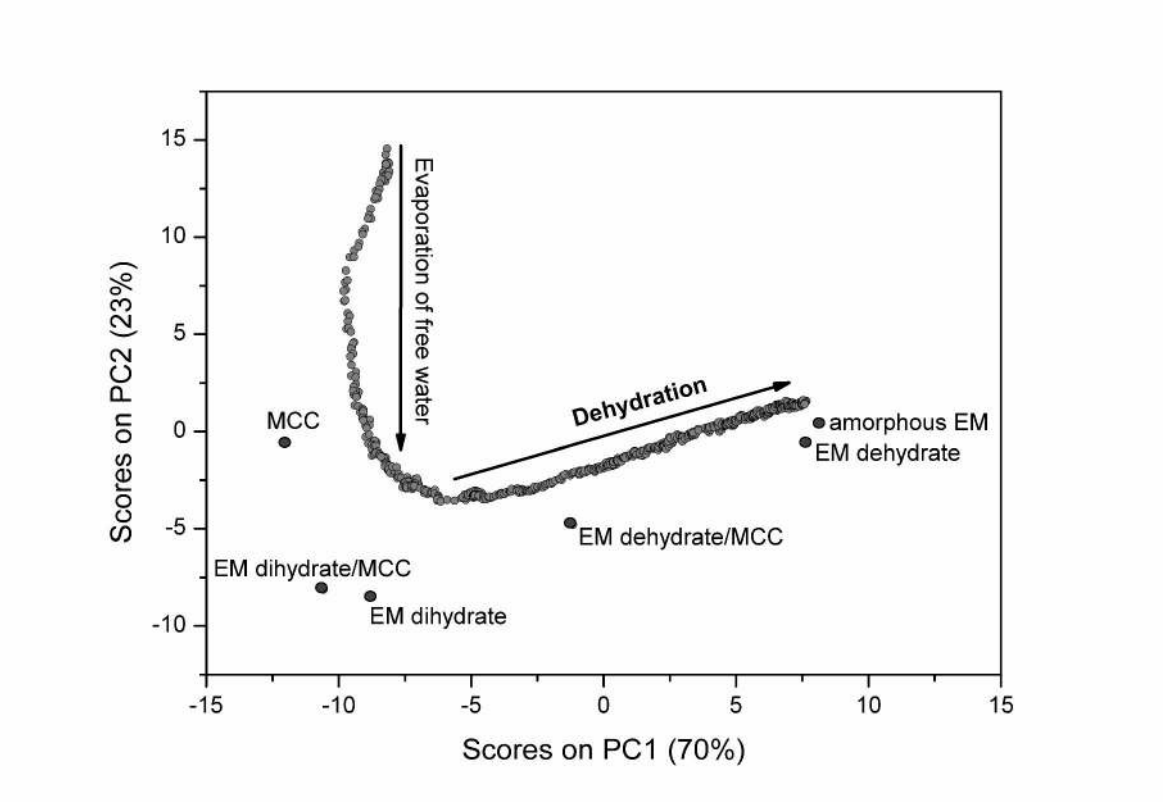

Figure 4. *Scores plot of the first principal components of pellets containing EM and MCC fluid-bed dried at 45°C (second batch). Principal component analysis of NIR spectra (first derivative, Savitzky-Golay smoothed, standard normal variate, mean centred).*

After ensuring that NIR spectroscopy is sensitive to the transformation of EM dihydrate into the isomorphic EM dehydrate, a diffuse reflectance NIR probe was used to monitor the fluid-bed drying process in-line. As presented in publication III, it was possible to detect dehydration of EM dihydrate for both batches dried at 60°C (Figure 5b, III) and for one batch dried at 45°C (Figure 4). For this purpose the wavelength range of 1360 to 2000 nm was selected. Further data pre-treatment included a Savitzky-Golay first derivative smoothing operation and normalisation using SNV correction. Finally the data was mean centred and PCA was performed. Only the first two PCs were used for this analysis combining between 86 to 95% of the variance. The first and the second PC were able to detect the structural differences between EM dehydrate and EM dihydrate. The third PC (about 2%) was mainly able to show that EM dihydrate, EM dehydrate, and amorphous EM exhibited

greater differences to the spectra of the pellets than the blends of EM dihydrate/MCC and EM dehydrate/MCC.

For the first part of the process the decreasing signal of the first overtone OH-stretching (Figure 5) marks the evaporation of the free and unbound water (first arrow). The second part of the process is dominated by the blueshift of the combination band of water from 1937 nm for EM dihydrate/MCC to 1926 nm for EM dehydrate/MCC (third arrow). This is a result of evaporation of the lattice bound water (Figure 4, III). These changes, as well as the appearance of the peaks between 1680 to 1730 nm (second arrow), are important wavelengths in the loadings plot of the first and second PCs (Figure 5c, III).

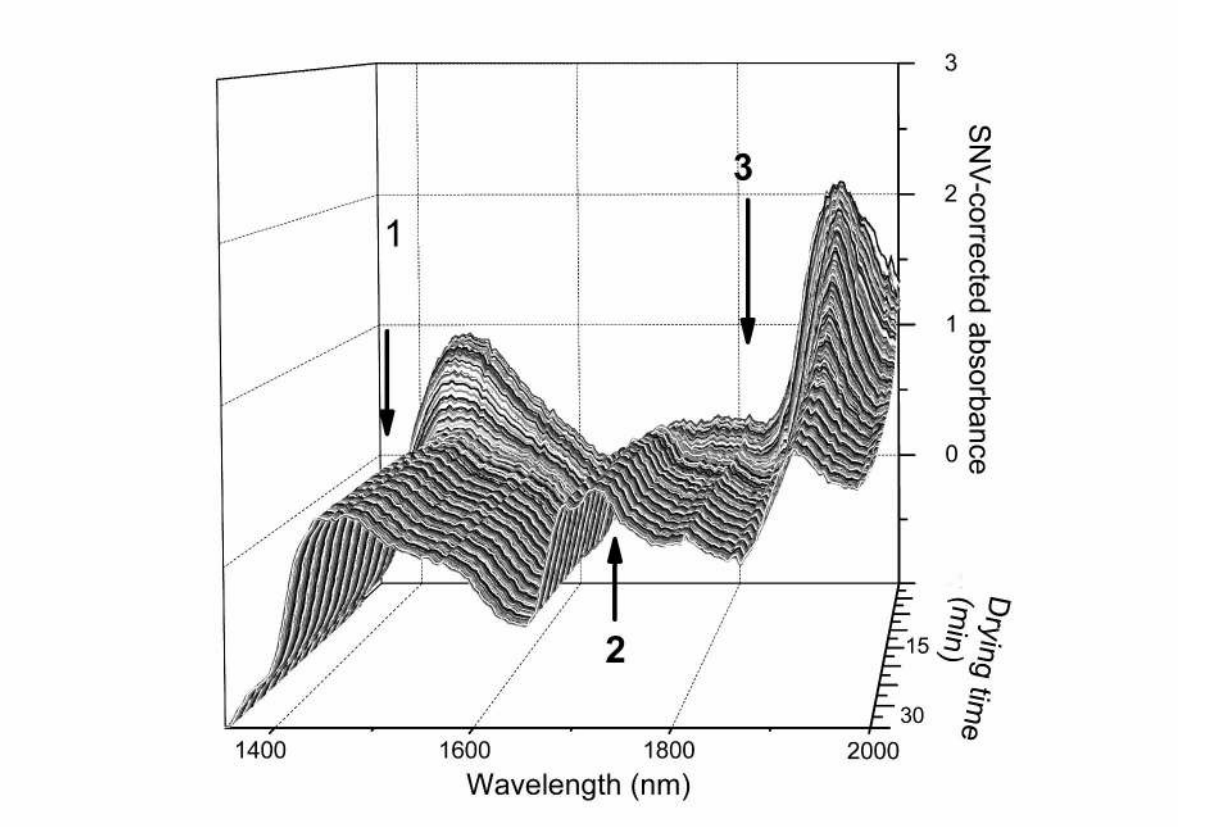

Figure 5. *Standard normal variate corrected near-infrared spectra of the fluid-bed drying process of the EM pellets dried at 60 °C (second batch).*

Though the first trace of EM dehydrate could not be detected using PCA analysis, the physical change in the evaporation process from free to chemically bound water is indicated by the change in slope in the PCA scores plot. Therefore, it enables suitable end-point detection of the drying process before the occurrence of EM dehydrate is evident.

5.5. Film coating process (IV)

Tablets containing high density polyethylene and Aerosil® 200 were coated using the rotating plate system. A detailed description of this set-up can be found in publication IV. These tablets, individually labelled, were coated with 5 to 25 plate rotations, resulting in different coating thicknesses of 25 to 400 µm. Each process was monitored by in-line NIR spectroscopy. Final spectra of each of the coated and dried tablets (n = 20) were taken and assigned to the corresponding coating thickness. The tablet thickness was measured before and after the coating process individually with a digital micrometer.

After selecting the wavelength range of 1160 to 1780 nm, the data was pre-processed using a smoothing operation (Savitzky-Golay), SNV correction, and MC. The data was divided into the calibration set and the test set. The calibration set was used to calculate the PLS regression model.

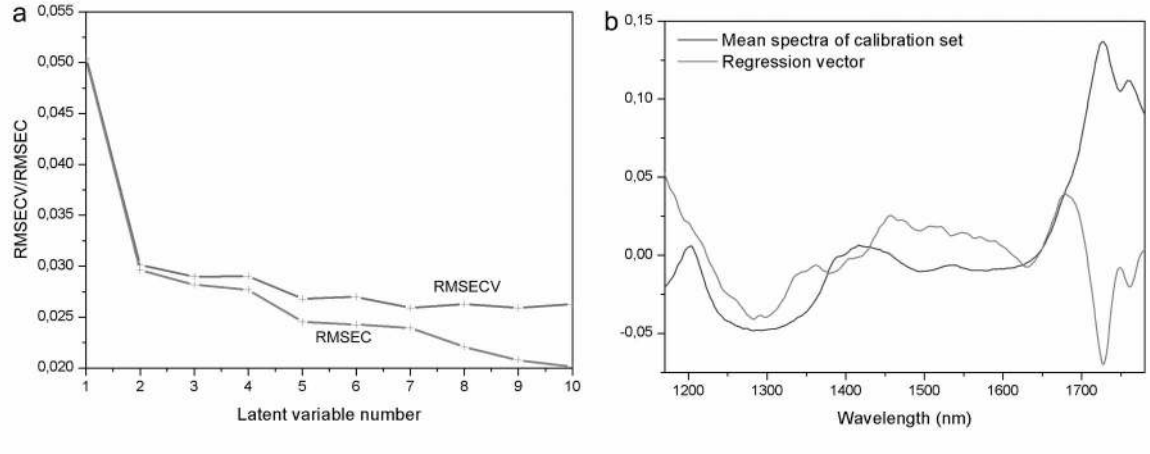

Figure 6. *PRESS-plot (a), regression vector of the partial least squares model, and the mean spectra of the calibration set (b).*

Three LVs were selected for the PLS regression model. The PRESS plot (Figure 6a) clearly indicated that three LVs were sufficient for the model. The regression vector (Figure 6b), that can be used to indicate model over-fitting by random variation, showed hardly any inclusion of noise when choosing three LVs. As presented in publication IV, the first LV (Figure 7a) represents the baseline changes attributable to an increase of particle size of the tablets and also a change in surface texture due to the coating.

In addition, the signal from the tablet core decreased with increased coating thickness according to the Beer Lambert law, and thus contributing to the changes in the baseline. The first LV has the greatest power to separate the data points according to their thickness. For the coating thickness prediction, however, the second LV, describing the chemical signal of the coating solution, and the third LV, showing the signal of the tablet core, are crucial.

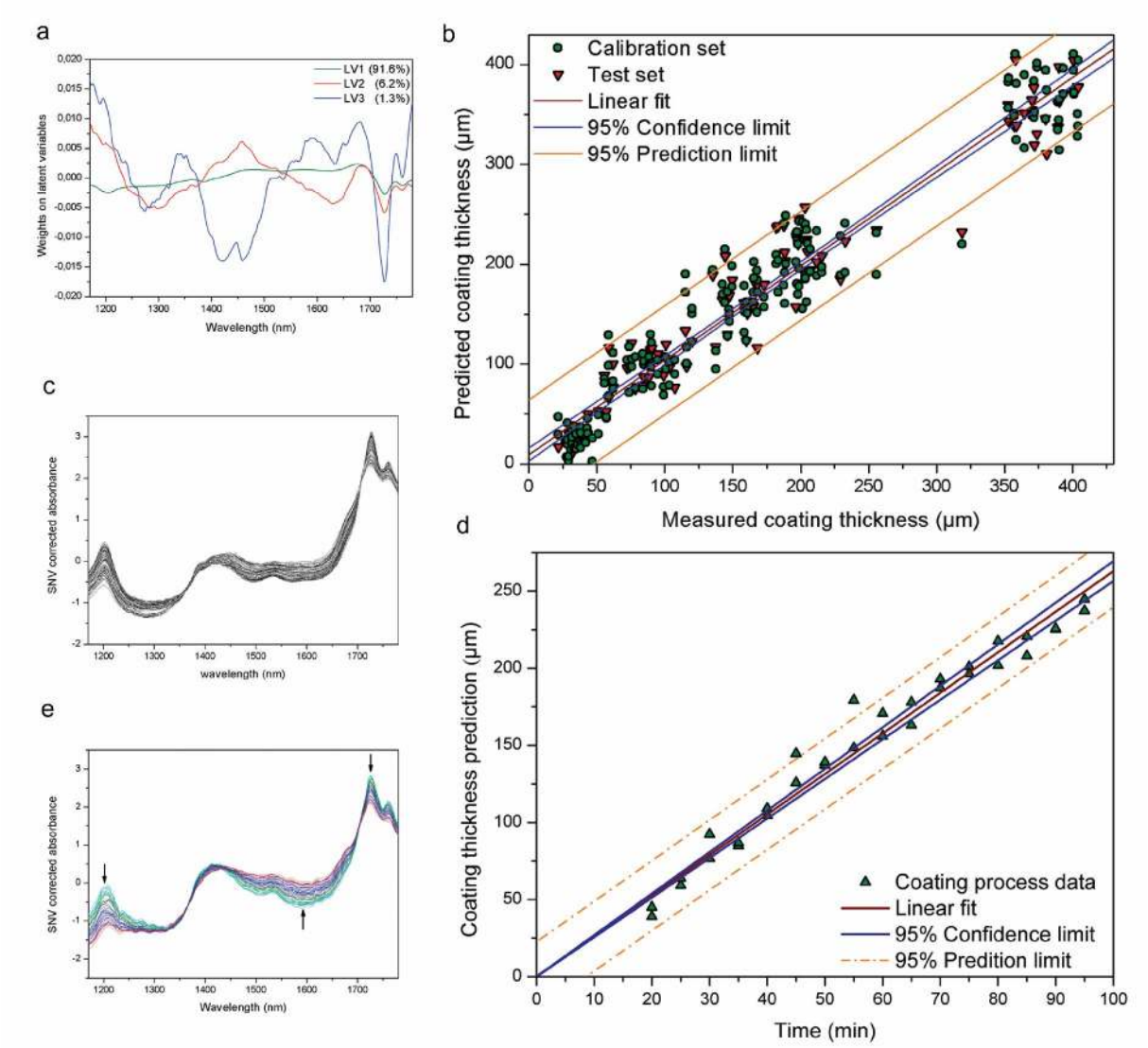

Figure 7. *The signals contributing to the LVs in the weights plot (a). Coating thickness prediction of the calibration and test set (b). Standard normal variate corrected spectra of the in-line near-infrared data obtain during the coating drum process (c). The standard normal variate corrected spectra from the rotating plate coating process (d). Coating thickness prediction (e) of in-line near-infrared data from the coating drum.*

The results of the cross validation showed a suitable prediction capacity when applied to the test set (RMSEC: 28.2 µm, RMSECV: 29.0 µm, RMSEP: 28.5 µm). When examining the influence plot (Figure 6b, IV), the samples with a coating thickness higher than 300 µm showed a generally negative Y-studentised residual, meaning the model predicted a lower coating thickness than measured. This showed the flaws of the model for predicting thicker coatings due to the limitations of the Beer Lambert law.

After calibrating and testing the PLS model (Figure 7b), the model was applied to data obtained by in-line NIR spectroscopy during a coating drum process. For this coating process the same tablet composition was used as for the rotating plate

system only the shape of the tablet cores differed. For the rotating plate system flat-faced tablets were more suitable because they allowed equal distribution of the coating solution. In contrast to this, biconvex tablets were required for the coating drum process to prevent the tablets from sticking together. The SNV corrected spectra of both processes (Figure 7c and e) contained many similarities, although there was more noise visible in the spectra obtained from the coating drum process.

The coating thickness prediction (Figure 7d) of the coating drum process resulted in a thickness of 240 µm while the digital micrometer measured 210 µm. The difference between the prediction of the PLS model and the measured coating layer thickness can be explained by the error of the digital micrometer (approximately 10%). For both measurements (before and after coating) this resulted in an error of about 30 µm thus the difference of 30 µm was within the error-limits. Coating quality differences were mainly due to the ineffective drying unit attached to the rotating plate and the wave-like pumping of the peristaltic pump used and may have added up to the error of the digital micrometer.

5.6. Analysis of the quality of coating (V)

At first, before the actual measurements of the coated tablets were performed, the refractive index (RI) of the coating system was determined. This was necessary for an accurate coating thickness calculation, but avoided the need for a calibration model to be developed. The coating thickness is calculated from the time delay between the surface reflection and the reflection from the interface of the coating and the tablet core; taking into account the speed of light and the refractive index (n) of the examined system. Thus, the RI of each solid component used in the coating solution was determined using TPS. The RI of the coating was estimated based on the weight percentage of each component in the coating. The calculated value of 1.85 roughly agreed with the RI value of 1.87 obtained from the coating on the tablet. The coating thickness calculations were based on the measured value of 1.87. Even without the determination of an accurate RI, it is still possible to extract information that enables one to compare batch-to-batch variability.

For the tablet coating quality analysis ten coated tablets were measured by TPI. The whole tablet was scanned at the laser gauge to create a surface model of both tablet sides and the central band. Based on this morphological model the 3D terahertz image was created by first scanning tablet side a, then the central band and finally tablet side b. The 3D terahertz image was constructed from terahertz waveforms, which contained all the information required to form the basis of a voxel of the tablet (Figure 1, V). The reflection from a tablet interface resulted in either a maximum (if the RI of the subsequent system was greater) or a minimum (if the RI of the subsequent system was smaller). These interfaces in this study were between: air/main coat (maximum: $n_{air} < n_{main\ coat}$), main coat/sub-coat (minimum: $n_{main\ coat} > n_{sub\text{-}coat}$) and sub-coat/tablet core (minimum $n_{sub\text{-}coat} > n_{core}$). Since the interface between the two coating layers and between sub-coat and tablet core both resulted

in a minimum and the thickness of the coat was under the diffraction limit of the TPI, it was not possible to resolve the two minima. The results show a broadened peak in the time domain wave form. Consequently, the thickness of the sub-coat could not be determined by TPI in this particular study.

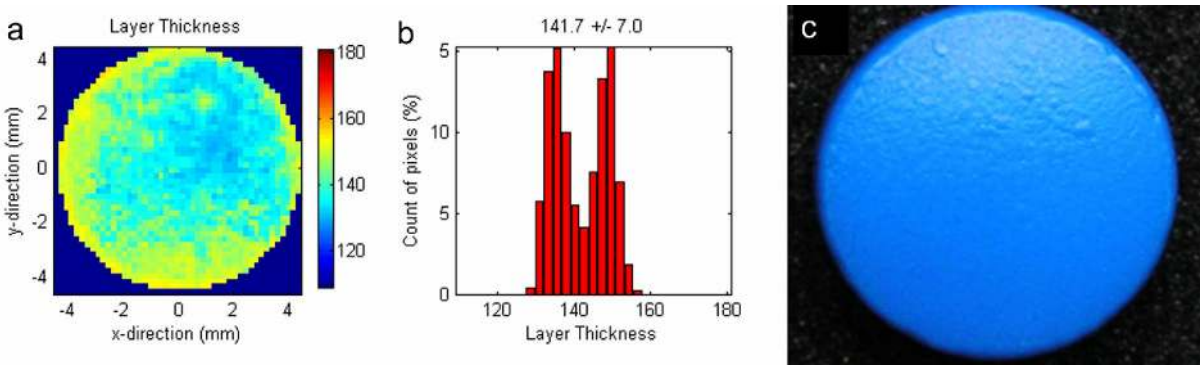

Figure 8. *False coloured image (a) of tablet side b reveals the coating thickness distribution. The histogram (b) shows the bimodal coating thickness on the tablet side. The unit scale is given in µm. The photograph taken of this tablet side is shown in (c).*

The average layer thickness of both tablet sides (sample 3) was 149 µm (Table 1, V) and comparable with the reference method – an optical microscope (a destructive method), which also resulted in an average thickness of 149 µm. The TPI 2D images on one tablet surface showed variability in the coating thickness. Tablet side b (Figure 8a) revealed a thickness varying between 148 µm at the edges and a minimum of 130 µm on the centre of the side b. The histogram of the layer thickness distribution (Figure 8b) showed bimodal thickness distribution (of about 136 µm and 152 µm) around the mean of 142 µm.

When observing the 3D image of the tablet side a and the central band (Figure 9a) two main conclusions can be drawn. Firstly, side a is obviously more evenly coated and has a thicker coating than tablet side b (average thickness side a: 152 µm). Secondly, the coating thickness of the central band is lower than the coating thickness of the tablet sides. The mean coating layer thickness of the central band of all ten tablets was found to be 33 % lower than the thickness of the tablet sides.

To compare the results for the measurements between the TPI and the optical microscope, a student's t-test was performed and showed good agreement between the two techniques (TPI and optical microscopy) on the measurements of coating layer thickness for the tablet sides (with a *p* value of 0.17). The tablet central band, on the other hand, showed a *p* value of 0.01 indicating greater variation between the two analytical methods due to greater terahertz signal scattering. This is a result of higher morphological curvature around the tablet central band.

Nevertheless, TPI has several advantages over optical microscopy. The greatest advantages are that it is a non-destructive method and able to give an image of the whole tablet. In addition, it provides fast detection of the coating distribution and the coating uniformity, which helps to reveal defects in the coating that are not visible to the naked eye (Figure 8c).

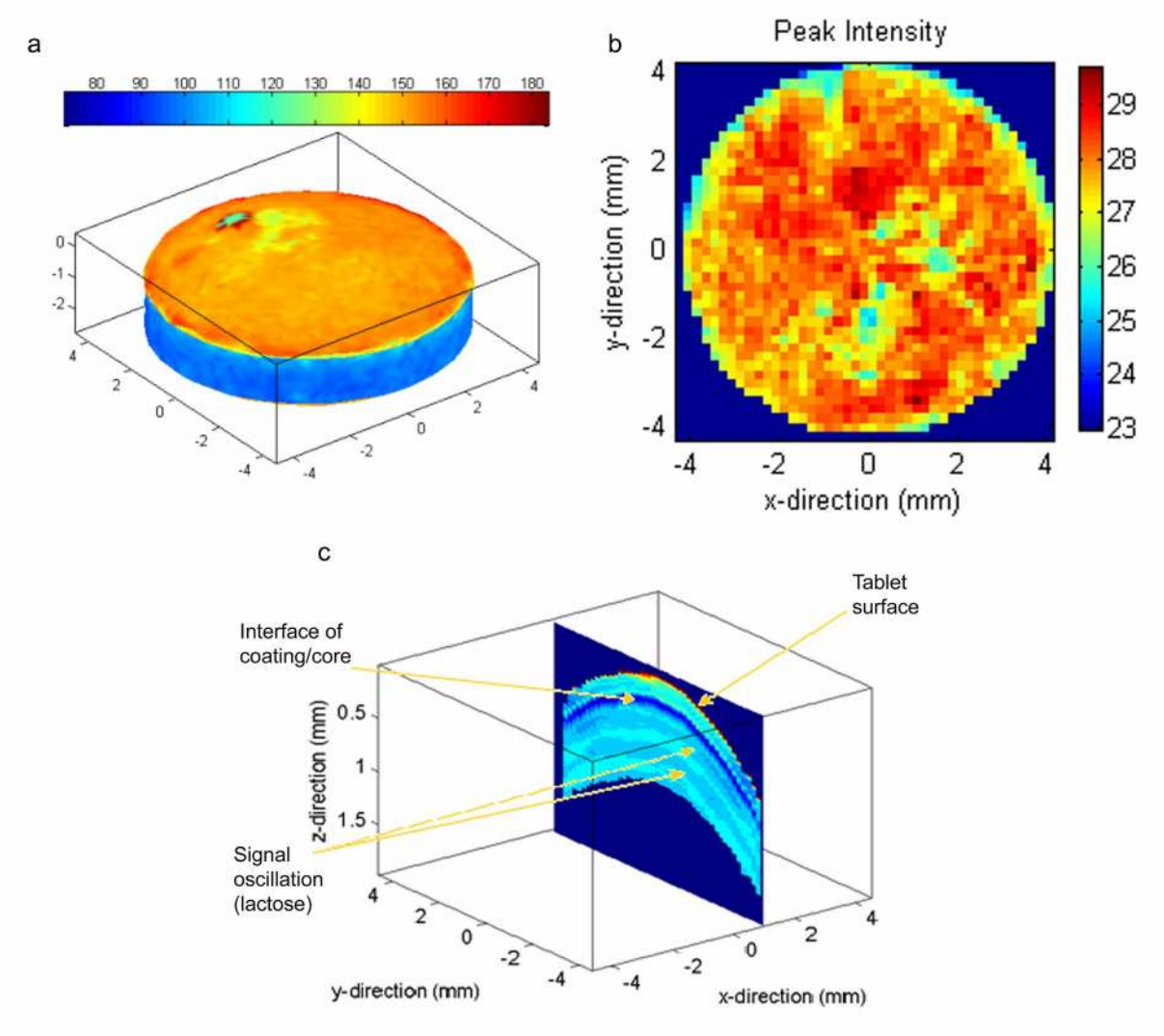

Figure 9. *3D image (a) of the tablet side a and the central band. The colour bar scale is in µm, the x, y and z axis give the dimensions of the tablet in mm. The peak intensity image (b) of tablet side b reconstructs the orange peel defects of the coating. The virtual cross section through the tablet (c) reveals the different interfaces.*

Another advantage is in the analysis of defects. The blister defect on tablet side a, which is visible in Figure 8a and c, was located by virtually slicing the image in the z-axis (Figure 7, V). The depth of the blister was determined to be 314 µm, exceeding the coating layer, and is obviously a tablet defect. By slicing the image in the x direction (Figure 5, V) the defect was localised and the diameter was determined to be 0.7 mm.

It was also possible to measure the surface roughness of the coating (orange peel defect) by determining the TEFPS. The red areas in the peak intensity map (Figure 9b) exhibit domains of smooth coating when the majority of the light emitted was reflected back or absorbed. If the pulse hits rougher areas of the coating a greater amount of the pulse will be scattered, leading to a decrease of the detected signal.

This is marked by the blue-green areas in Figure 9b. When examining the surface roughness, the RI was found to be proportional to the reflectivity and varied over the surface of the coated tablet. Due to the different methods in measuring the coating thickness and the surface roughness, the coating thickness determination was not affected by the intensity changes due to the surface roughness.

6. Summary and conclusions

Vibrational spectroscopy has been used to gain insight into process-induced transformations. Monitoring the blending of a three component system by near-infrared (NIR) spectroscopy provided information about the blend homogeneity, thus making it possible to determine the end point of the blending process. Hydrate formation was observed by Raman spectroscopy for nitrofurantoin and theophylline during pelletisation. NIR spectroscopy was not able to detect any changes during this processing step due to the strong signal of the water used as granulation liquid. For erythromycin dihydrate it was not possible to detect any solid-state changes by either technique. Dehydration was detected at-line with XRPD and Raman spectroscopy for nitrofurantoin and theophylline. Being sensitive to hydrogen bonding changes NIR spectroscopy was successfully used to follow the dehydration for all three drugs under investigation. It was even possible to detect the formation of an isomorphic dehydrate of erythromycin during a fluid-bed drying process using in-line NIR spectroscopy in combination with principal component analysis.

To study coatings, NIR spectroscopy was used to monitor a small-scale rotating plate coating process, and a calibration model was developed using partial least squares regression. This model was then used to predict the coating thickness of tablets of the same core composition, coated with the same coating solution, but coated in a regular coating pan. The prediction was just within the error limits but reducing the errors will result in better data, and thus enable a better prediction.

Terahertz pulsed imaging, used to examine sustained-release coated tablets, was able to assess the coating layer thickness, distribution, reproducibility, and uniformity. Due to the possibility of producing 3D images of the measured tablet, the technique can be used to localise and quantify coating defects.

It can, therefore, be concluded that vibrational spectroscopy based tools were suitable for monitoring different production steps at-line as well as in-line. The increase in process understanding may enable modelling physico-chemical phenomena that occur under specific conditions. This will greatly improve the quality of pharmaceutical products and, in the long run, may have a contribution to the development of novel techniques for pharmaceutical production and new applications.

References

Aaltonen J., Heinänen P., Peltonen L., Kortejärvi H., Tanninen V.-P., Christiansen L., Hirvonen J., Yliruusi J., Rantanen J. (2006) In situ measurement of solvent-mediated phase transformations during dissolution testing. *Journal of Pharmaceutical Sciences* **95** (12): 2710-2736.

Aaltonen J., Strachan C. J., Pöllänen K., Yliruusi J., Rantanen J. (2007a) Hyphenated spectroscopy as a polymorph screening tool. *Journal of Pharmaceutical and Biomedical Analysis* **44** (2): 477-483.

Aaltonen J., Kogerman K., Strachan C. J., Rantanen J. (2007b) In-line monitoring of solid-state transitions during fluidisation. *Chemical Engineering Science* **62** (1-2): 408-415.

Abrahamsson C., Johansson J., Andersson-Engels S., Svanberg S., Folestad S. (2005) Time-resolved NIR spectroscopy for quantitative analysis of intact pharmaceutical tablets. *Analytical Chemistry* **77** (4): 1055-1059.

Airaksinen S., Luukkonen P., Jørgensen A., Karjalainen M., Rantanen J., Yliruusi J. (2003) Effects of excipients on hydrate formation in wet masses containing theophylline. *Journal of Pharmaceutical Sciences* **92**: 616-528.

Airaksinen S., Karjalainen M., Räsänen E., Rantanen J., Yliruusi J. (2004) Comparison of the effect of two drying methods on polymorphism of theophylline. *International Journal of Pharmaceutics* **276**: 129-141.

Allis D. G., Korter T. M. (2006) Theoretical analysis of the terahertz spectrum of the high explosive PETN. *ChemPhysChem* **7** (11): 2398-2408.

Amado A. M., Nolasco M. M., Ribeiro-Claro P. J. A. (2007) Probing pseudopolymorphic transitions in pharmaceutical solids using Raman spectroscopy: Hydration and dehydration of theophylline. *Journal of Pharmaceutical Sciences* **96** (5): 1366-1379.

Andersson M., Josefson M., Langkilde F. W., Wahlund K. G. (1999) Monitoring of a film coating process for tablets using near infrared reflectance spectrometry. *Journal of Pharmaceutical and Biomedical Analysis* **20**: 27-37.

Andersson M., Folestad S., Gottfries J., Johansson M. O., Josefson M., Wahlund K. G. (2000) Quantitative analysis of film coating in a fluidized bed process by in line NIR spectrometry and multivariate batch calibration. *Analytical Chemistry* **72** (9): 2099-2108.

Bakeev K. A. (2003) Near-infrared Spectroscopy as a process analytical tool. *Pharmaceutical Technology Europe*, September 2003.

Barnes R. J., Dhanoa M. S., Lister S. J. (1989) Standard normal variate transformation and de-trending of near-infrared diffuse reflectance spectra. *Applied Spectroscopy* **43** (5): 772-777.

Bauer J. F., Dziki W., Quick J. E. (1999) Role of an isomorphic desolvate in dissolution failures of an erythromycin tablet formulation. *Journal of Pharmaceutical Sciences* **88** (11): 1222-1227.

Baughman E. (2005) Process analytical chemistry: Introduction and historical perspective. Process analytical technology: Spectroscopic tools and

implementation strategies for the chemical and pharmaceutical industries. K. A. Bakeev, Editor. Oxford. Blackwell Publishing: pp. 1-11.

Bechtloff B., Nordhoff S., Ulrich J. (2001) Pseudopolymorphs in industrial use. *Crystal Research and Technology* **39** (12): 1315-1328.

Beebe K. R., Blaser W. W., Bredeweg R. A., Chauvel J. P., Harner R. S., LaPack M., Leugers A., Martin D. P., Wright L. G., Yalvact E. D. (1993) Process analytical chemistry. *Analytical Chemistry* **65**: 199-216.

Berntsson O., Zackrisoon G., Östling G. (1997) Determination of moisture in hard gelatine capsules using near-infrared spectroscopy: applications to at-line process control of pharmaceutics. *Journal of Pharmaceutical and Biomedical Analysis* **15**: 895-900.

Blanco M., Coello J., Eustaquio A., Iturriaga H., Maspoch S. (1999) Analytical control of pharmaceutical production steps by near infrared reflectance spectroscopy. *Analytica Chimica Acta* **392** (2-3): 237-246.

Blanco M., Coello J., Iturriaga H., Maspoch S., Pou N. (2000) Development and validation of a near infrared method for the analytical control of a pharmaceutical preparation in three steps of the manufacturing process. *Fresenius Journal of Analytical Chemistry* **368** (5): 534-539.

Blanco M., Valdes D., Llorente I., Bayod M. (2005) Application of NIR spectroscopy in polymorphic analysis: Study of pseudo-polymorphs stability. *Journal of Pharmaceutical Sciences* **94** (6): 1336-1342.

Blanco M., Bautista M., Alcalá M. (2008) Preparing calibration sets for use in pharmaceutical analysis by NIR-spectroscopy. *Journal of Pharmaceutical Sciences* **97** (3): 1236-1245.

Brereton R. G. (2005) Chemometrics and PAT. *PAT Journal* **2** (3): 8-11.

Buckton G., Yonemochi E., Hammond J., Moffat A. (1998) The use of near infra-red spectroscopy to detect changes in the form of amorphous and crystalline lactose. *Journal of Pharmaceutical Sciences* **168** (2): 231-241.

Burger A., Ramberger R. (1979) On polymorphism of pharmaceuticals and other molecular crystals. II. *Mikrochimica Acta* **2** (3-4): 273-316.

Byrn S. R., Xu W., Newman A. W. (2001) Chemical reactivity in solid-state pharmaceuticals: formulation implications. *Advanced Drug Delivery Reviews* **48** (1): 115-136.

Chalus P., Walter S., Ulmschneider M. (2007) Combined wavelet transform -artificial neural network use in tablet active content determination by near-infrared spectroscopy. *Analytica Chimica Acta* **591**: 219-224.

Ciurczak E. W., Torlini R. P., Demkowicz M. P. (1986) Determination of particle size of pharmaceutical raw materials using near infrared reflectance spectroscopy. *Spectroscopy* **1**: 36-39.

Coates J. (2000) Interpretation of infrared spectra, a practical approach. Encyclopaedia of Analytical Chemistry R. A. Meyers, Editor. Chichester. John Wiley & Sons, Ltd, pp. 10815-10837.

Cogdill R. P., Anderson C. A., Delgado-Lopez M., Molseed D., Chisholm R., Bolton R., Herkert T., Afnán A. M., Drennen J. K. (2005a) Process analytical technology case study Part I: Feasibility studies for quantitative near-infrared method development. *AAPS PharmSciTech* **6** (2): article 37.

Cogdill R. P., Anderson C. A., Delgado M., Chisholm R., Bolton R., Herkert T., Afnán A. M., Drennen J. K. (2005b) Process analytical technology case study Part II: Development and validation of quantitative near-infrared calibrations in support of a process analytical technology application for real-time release. *AAPS PharmSciTech* **6** (2): article 38.

Cogdill R. P., Anderson C. A., Drennen J. K. (2005c) Process analytical technology case study Part III: Calibration monitoring and transfer. *AAPS PharmSciTech* **6** (2): article 39.

Crawley D., Longbottom C., Wallace V. P., Cole B., Arnone D., Pepper M. (2003) Three dimensional terahertz pulsed imaging of dental tissue. *Journal of Biomedicine Optics* **8**: 303-307.

Crucio J. A., Petty C. C. (1951) The near infrared absorption spectrum of liquid water. *Journal of the Optical Society of America* **41**: 302-304.

Datta S., Grant D. W. J. (2004) Crystal structures of drugs: Advances in determination, prediction and engineering. *Nature Reviews Drug Discovery* **3**: 42-47.

Day G. M., Zeitler J. A., Jones W., Rades T., Taday P. F. (2006) Understanding the influence of polymorphism on phonon spectra: Lattice dynamics calculations and terahertz spectroscopy of carbamazepine, *Journal of Physical Chemistry* B **110** (1): 447-456.

de Juan A., Tauler R. (2003) Chemometrics applied to unravel multicomponent processes and mixtures. Revisiting the latest trends in multivariate resolution. *Analytica Chimica Acta* **500**: 195-210.

de Juan A., Tauler R. (2006) Multivariate curve resolution (MCR) from 2000: Progress in concepts and applications. *Critical Reviews in Analytical Chemistry* **36** (3-4): 163-176.

Doherty S. J., Lange A. J. (2006) Avoiding pitfalls with chemometrics and PAT in the pharmaceutical and biotech industries. *Trends in Analytical Chemistry* **25** (11): 1097-1102.

EMEA European Medicines Agency (2003) Note for guidance on the use of near infrared spectroscopy. www.emea.europa.eu/pdfs/human/qwp/330901en.pdf 2003.

FDA, Food and Drug Administration (2004a) Guidance for industry PAT – A framework for innovative pharmaceutical manufacturing and quality assurance. http://www.fda.gov/CDER/guidance/6419fnl.pdf.

FDA, Food and Drug Administration (2004b) Pharmaceutical cGMPs for the 21st century – risk based approach. www.fda.gov/cder/gmp/gmp2004/GMP_final report2004.htm.

Ferguson B., Zhang X-C. (2002) Materials for terahertz science and technology. *Nature Materials* **1**(1): 26-33.

Fernandez F. M., Green M. D., Newton P. N. (2008) Prevalence and detection of counterfeit pharmaceuticals: A mini review. *Industrial & Engineering Chemistry Research* **47** (3): 585-590.

Févotte G., Calas J., Puel F., Hoff C. (2004) Applications of NIR spectroscopy to monitoring and analyzing the solid state during industrial crystallization processes. *International Journal of Pharmaceutics* **273** (1-2): 159-169.

Fitzgerald A. J., Cole B. E., Taday P. F. (2005) Non-destructive analysis of tablet coating thicknesses using terahertz pulsed imaging. *Journal of Pharmaceutical Sciences* **94** (1): 177-183.

Foley W. J., McIlwee A., Lawler I., Aragones L., Woolnough A. P., Berding N. (1998) Ecological applications of near infrared reflectance spectroscopy – a tool for rapid, cost-effective prediction of the composition of plant and animal tissue and aspects of animal performance. *Oecologia* **116**: 293-305.

Fountain W., Dumstorf K., Lowell A. E., Lodder R. A., Mumper R. J. (2003) Near-infrared spectroscopy for determination of testosterone in thin-film composites. *Journal of Pharmaceutical and Biomedical Analysis* **33**: 181-189.

Galway A. K. (2000) Structure and order in thermal dehydrations of crystalline solids. *Thermochimica Acta* **355**: 181-238.

Gandhi R., Pillai O., Thilagavathi R., Gopalakrishnan B., Kaul C. L., Panchagnula R. (2002) Characterization of azithromycin hydrates. *European Journal of Pharmaceutical Sciences* **16** (3): 175-184.

Garnier S., Petit S., Coquerel G. (2002) Dehydration mechanism and crystallisation behaviour of lactose. *Journal of Thermal Analysis and Calorimetry* **68**: 489-502.

Giron D. (1995) Thermal analysis and calorimetric methods in the characterisation of polymorphs and solvates. *Thermochimica Acta* **248**: 1-59.

Giron D., Goldbronn C., Mutz M., Pfeffer S., Piechon P., Schwab P (2002) Solid-state characterisations of pharmaceutical hydrates. *Journal of Thermal Analysis and Calorimetry* **68**: 453-465.

Giron D., Mutz M., Garnier S. (2004) Solid-state of pharmaceutical compounds. Impact of the ICH Q6 guideline on industrial development. *Journal of Thermal Analysis and Calorimetry* **77**: 709-747.

Giron D., Monnier S., Mutz M., Piechon P., Buser T., Stowasser F., Schulze K., Bellus M. (2007) Comparison of quantitative methods for analysis of polyphasic pharmaceuticals. *Journal of Thermal Analysis and Calorimetry* **89** (3): 729-743.

Gradinarsky L., Johansson J., Claybourn M., Yang H., Ahlqvist M., Folestad S. (2006) Terahertz spectroscopy – New opportunities for understanding. *European Pharmaceutical Review* **3**: 77-83.

Grant D. J. W. (1999) Theory and origin of polymorphism. Polymorphism in pharmaceutical solids. H. G. Brittain, Editor. New York, Marcel Dekker, Inc. pp. 1-35.

Gupta A., Peck G. E., Miller R. W., Morris K. R. (2005) Real-time near-infrared monitoring of content uniformity, moisture content, compact density, tensile strength, and Young's modulus of roller compacted powder blends. *Journal of Pharmaceutical Sciences* **94** (7): 1589-1597.

Hailey P. A., Doherty P., Tapsell P., Oliver T., Aldridge P. K. (1996) Automated system for on-line monitoring of powder blending processes using near-infrared spectroscopy Part I. System development and control. *Journal of Pharmaceutical and Biomedical Analysis* **14**: 551-559.

Halebian J. K., McCrone W. (1969) Pharmaceutical applications of polymorphism. *Journal of Pharmaceutical Sciences* **58** (8): 911-929.

Harris R. K., Ghi P. Y., Puschmann H., Apperley D. C., Griesser U. J., Hammond R. B., Ma C., Roberts K. J., Pearce G. J., Yates J. R., Pickard C. J. (2005) Structural

studies of polymorphs of carbamazepine, its dihydrate, and two solvates. *Organic Process Research & Development* **9**: 902-910.

Hausman D. S., Cambron R. T., Sakr A. (2005) Application of on-line Raman spectroscopy for characterizing relationships between drug hydration state and tablet physical stability. *International Journal of Pharmaceutics* **299** (1-2): 19-33.

Heinz A., Strachan C. J., Atassi F, Gordon K. C., Rades T. (2008) Characterising an amorphous system exhibiting trace crystallinity: A case study with saquinavir. *Crystal Growth & Design* **8** (1): 119-127.

Heise H. M., Winzen R. (2002) Chemometrics in near-infrared spectroscopy. Near-infrared spectroscopy. Principles, instruments, applications. H.W. Siesler, Editor. Weinheim, WILEY-VCH Verlag GmbH, pp. 125-159.

Herman J., Remon J. P., Visavarungroj N., Schwartz J. B., Klinger G. H. (1988) Formation of theophylline monohydrate during the pelletisation of microcrystalline cellulose – anhydrous theophylline blends. *International Journal of Pharmaceutics* **42** (1-3):15-18.

Ho L., Müller R., Gordon K., Kleinebudde P., Pepper M., Rades T., Shen Y., Taday P., Zeitler J. A. (2008) Applications of terahertz pulsed imaging to sustained-release tablet film coating quality assessment and dissolution performance. *Journal of Controlled Release* doi: 10.1016/j.jconrel.2008.01.002.

Hoppu P., Jouppila K., Rantanen J., Schantz S., Juppo A. M. (2007) Characterisation of blends of paracetamol and citric acid. *Journal of Pharmacy and Pharmacology* **59** (3): 373-381.

Huang H., Yu H., Xu H., Ying Y. (2008) Near infrared spectroscopy for on/in-line monitoring of quality in foods and beverages: A review. *Journal of Food Engineering* **87**: 303-313.

ICH International Conference on Harmonisation (1999) ICH Q6b Guideline specification: Test procedures and acceptance criteria for new drug substances and new drug products: Chemical substances. http://www.ich.org/LOB/media/MEDIA430.pdf.

ICH International Conference on Harmonisation (2007) ICH Q8a Pharmaceutical development. http://www.ich.org/LOB/media/MEDIA1707.pdf annex: http://www.ich.org/LOB/media/MEDIA4349.pdf.

ICH International Conference on Harmonisation (2005) ICH Q9 Quality risk management. http://www.ich.org/LOB/media/MEDIA1957.pdf.

Jakobsen R. J., Brasch J. W., Mikawa Y. (1968) Past results and future prospects of far infrared studies of hydrogen bonding. *Applied Spectroscopy* **22** (6): 641-649.

Johansson J., Petterson S., Folestad S. (2002) Infrared imaging of laser-induced heating during Raman spectroscopy of pharmaceutical solids. *Journal of Pharmaceutical and Biomedical Analysis* **30** (4): 1223-1231.

Johansson J., Petterson S., Folestad S. (2005) Characterisation of different laser irradiation methods for quantitative Raman tablet assessment. *Journal of Pharmaceutical and Biomedical Analysis* **39**: 510-516.

Johansson J., Sparén A., Svensson, O., Folestad, S., Claybourn, M. (2007) Quantitative transmission Raman spectroscopy of pharmaceutical tablets and capsules. *Applied Spectroscopy* **61**(11): 1211-1218.

Jørgensen A. C., Rantanen J., Karjalainen M., Khriachtchev L., Räsänen E., Yliruusi J. (2002) Hydrate formation during wet granulation studied by spectroscopic methods and multivariate analysis. *Pharmaceutical Research* **19** (9): 1285-1291.

Jørgensen A. C., Luukkonen P., Rantanen J., Schæfer T., Juppo A. M., Yliruusi J. (2004) Comparison of torque measurements and near-infrared spectroscopy in characterisation of wet granulation process. *Journal of Pharmaceutical Sciences* **93** (9): 2232-2243.

Jørgensen A. C., Miroshnyk I., Karjalainen M., Jouppila K., Siiria S., Antikainen O., Rantanen J. (2006) Multivariate data analysis as a fast tool in evaluation of solid-state phenomena. *Journal of Pharmaceutical Sciences* **95** (4): 906-916.

Karjalainen M., Airaksinen S., Rantanen J., Aaltonen J., Yliruusi J. (2005) Characterisation of polymorphic solid-state changes using variable temperature X-ray powder diffraction. *Journal of Pharmaceutical and Biomedical Analysis* **39**: 27-32.

Kauffman J. F., Dellibovi M., Cunningham C. R. (2007) Raman spectroscopy of coated pharmaceutical tablets and physical models for multivariate calibration to tablet coating thickness. *Journal of Pharmaceutical and Biomedical Analysis* **43** (1): 39-48.

Kirsch J. D., Drennen J. K. (1995) Determination of film-coated tablet parameters by near-infrared spectroscopy. *Journal of Pharmaceutical and Biomedical Analysis* **13** (10): 1273-1281.

Kirsch J. D., Drennen J. K. (1996) Near-infrared spectroscopic monitoring of the film coating process. *Pharmaceutical Research* **13** (2): 234-237.

Kishi A., Otsuka M., Matsuda Y. (2002) The effect of humidity on dehydration behaviour of nitrofurantoin monohydrate studied by humidity controlled simultaneous instrument for X-ray diffractometry and differential scanning calorimetry (XRD-DSC). *Colloids and Surfaces B: Biointerfaces* **25**: 281-291.

Khankari R. K., Grant D. J. W. (1995) Pharmaceutical hydrates. *Thermochimica Acta* **248**: 61-79.

Kogermann K., Zeitler J. A., Rantanen J., Taday P.F., Pepper M., Heinämäki J., Strachan C. J. (2007) Investigating dehydration from compacts using terahertz pulsed, Raman and near-infrared spectroscopy. *Applied Spectroscopy* **61** (12): 1265-1274.

Kobayashi Y., Ito S., Itai S., Yamamoto K. (2000) Physicochemical properties and bioavailability of carbamazepine polymorphs and dihydrate. *International Journal of Pharmaceutics* **193**: 137–146.

Lachenal G. (1995) Dispersive and Fourier transform near-infrared spectroscopy of polymeric materials. *Vibrational Spectroscopy* **9**: 93-100.

Lavine B., Workman J. (2006) Chemometrics. *Analytical Chemistry* **78** (12): 4137-4145.

Lehto V.-P., Tenho M., Vaha-Heikkila K., Harjunen P., Paallysaho M., Valissaari J., Niemela P., Jarvinen K. (2006) The comparison of seven different methods to quantify the amorphous content of spray dried lactose. *Powder Technology* **167** (2): 85-93.

Li Y., Chow P. S., Tan R. B. H., Black S. N. (2008) Effect of water activity on the transformation between hydrate and anhydrate of carbamazepine. *Organic Process Research & Development* **21**: 264-270.

Luthra S. A., Hodge I. M., Pikal M. J. (2008) Investigation of the impact of annealing on global molecular mobility in glasses: Optimization for stabilization of amorphous pharmaceuticals. *Journal of Pharmaceutical Sciences* DOI 10.1002/jps.21255

Lypaert J., Massart D. L., Vander Heyden Y. (2007) Near-infrared spectroscopy applications in pharmaceutical analysis. *Talanta* **72**: 865-883.

Mark H., Workman J. (2003a) Derivatives in spectroscopy Part I – Behaviour of the derivative. *Spectroscopy* **18** (4): 32-37.

Mark H., Workman J. (2003b) Derivatives in spectroscopy Part II – The true derivative. *Spectroscopy* **18** (9): 25-28.

Mark H., Workman J. (2003c) Derivatives in spectroscopy Part III – Computing the derivative. *Spectroscopy* **18** (12): 106-111.

Mark H., Workman J. (2004) Derivatives in spectroscopy Part IV – Calibrating with derivatives. *Spectroscopy* **19** (1): 44-51.

Matousek P., Parker A.W. (2006) Bulk Raman analysis of pharmaceutical tablets. *Applied Spectroscopy* **60** (12): 1353-1357.

McCreery R. L. (2000) Raman spectroscopy for chemical analysis. New York, Wiley-Interscience.

Meada H., Ozaki Y., Tanaka M., Hayashi N., Kojima T. (1995) Near infrared spectroscopy and chemometrics studies of temperature-dependent spectral variations of water: relationship between spectral changes and hydrogen bonds. *Journal of Near Infrared Spectroscopy* **3**: 191-201.

Miroshnyk I., Khriachtchev L., Mirza S., Rantanen J., Heinämäki J., Yliruusi J. (2006) Insight into thermally induced phase transformations of erythromycin A dihydrate. *Crystal Growth & Design* **6** (2): 369-374.

Mirza S., Miroshnyk I., Heinämäki J., Christiansen L., Karjalainen M., Yliruusi J. (2003) Influence of solvents on the variety of crystalline forms of erythromycin. *AAPS PharmSciTech* **5** (2): article 12.

Mirza S., Heinämäki J., Miroshnyk I., Rantanen J., Christiansen L., Karjalainen M., Yliruusi J. (2006) Understanding processing-induced phase transformations in erythromycin – PEG 6000 solid dispersions. *Journal of Pharmaceutical Sciences* **95** (8):1723-1732.

Morris K. R., Nail S. L., Peck G. E., Byrn S. R., Griesser U. J., Stowell J. G., Hwang S-J., Park K. (1998) Advances in pharmaceutical materials and processing. *Pharmaceutical Science & Technology Today* **1**: 235-245.

Morris K. R. (1999) Structural aspects of hydrates and solvates. Polymorphism in pharmaceutical solids. H. G. Brittain, Editor. New York, Marcel Dekker, Inc: pp. 126-179.

Morris K. R., Griesser U. J., Eckhardt C. J. Stowell J. G. (2001) Theoretical approaches to physical transformations of active pharmaceutical ingredients during manufacturing processes. *Advanced Drug Delivery Reviews* **48** (1): 91-114.

Newnham D. A., Taday P. F. (2008) Pulsed terahertz attenuated total reflection spectroscopy. *Applied Spectroscopy* **62** (4): 96-112.

Norris K., Williams P. (1983) Optimisation of mathematical treatment of raw near-infrared signal in measurement of protein in hard red spring wheat. I. Influence of particle size. *Cereal Chemistry* **61**: 158-165.

Okumura T., Otsuka M. (2005) Evaluation of the microcrystallinity of a drug substance, indomethacin, in a pharmaceutical model tablet by chemometric FT-Raman spectroscopy. *Pharmaceutical Research* **22**: 1350-1357.

O'Neil A., Jee R., Moffat A. (1999) Measurement of the cumulative particle size distribution of microcrystalline cellulose using near infrared reflectance spectroscopy. *Analyst* **124**: 33-36.

Otsuka M., Kaneniwa N., Kawakami K., Umezawa O. (1990) Effect of surface characteristics of theophylline anhydrate powder on hygroscopic stability. *Journal of Pharmacy and Pharmacology* **42** (9): 606-610.

Otsuka M., Matsuda Y. (1994) The effect of humidity on hydration kinetics of mixtures of nitrofurantoin anhydride and diluents. *Chemical & Pharmaceutical Bulletin* **42**: 156-159.

Otsuka M. (2004) Comparative particle size determination of phenacetin bulk powder by using Kubelka-Munk theory and principal component regression analysis based on near infrared spectroscopy. *Powder Technology* **141**: 244-250.

Perez-Ramos J. D., Findlay W. P., Peck G., Morris K. R. (2005) Quantitative analysis of film coating in a pan coater based on in-line sensor measurements. *AAPS PharmSciTech* **6** (1): article 20.

Petit S., Coquerel G. (1996) Mechanism of several solid-solid transformations between dihydrate and anhydrous copper (II) 8-hydroxyquinolinates. Proposition of a unified model for the dehydration of molecular crystals. *Chemistry of Materials* **8**: 2247-2258.

Petit S., Mallet F., Petit M.-N., Coquerel G. (2007) Role of structural and macrocrystalline factors in the desolvation behaviour of cortisone acetate solvates. *Journal of Thermal Analysis and Calorimetry* **90**(1): 39-47.

Phadnis N. V., Suryanarayanan R. (1997) Polymorphism in anhydrous theophylline implications on the dissolution rate of theophylline tablets. *Journal of Pharmaceutical Sciences* **86**: 1256-1263.

Ph. Eur. (2008a) Thermal analysis. European Pharmacopoeia 6.1. Strasbourg France, Council of Europe: 01/2008: 20234.

Ph. Eur. (2008b) Characterisation of crystalline and partly crystalline solids by X-ray powder diffraction XRPD. European Pharmacopoeia 6.1. Strasbourg France, Council of Europe: 01/2008: 20933.

Ph. Eur. (2008c) Absorption spectrophotometry infrared. European Pharmacopoeia 6.1. Strasbourg France, Council of Europe: 01/2008: 20224.

Ph. Eur. (2008d) Near-infrared spectrophotometry. European Pharmacopoeia 6.1. Strasbourg France, Council of Europe: 01/2008: 20240.

Ph. Eur. (2008e) Raman spectrophotometry. European Pharmacopoeia 6.1. Strasbourg France, Council of Europe: 01/2008: 20248.

Pienaar E.W., Caira M.R., Lotter A.P. (1993a) Polymorphs of nitrofurantoin. 1. Preparation and X-ray crystal structures of two monohydrated forms of

nitrofurantoin. *Journal of Crystallographic and Spectroscopic Research* **23**: 739-744.

Pienaar E.W., Caira M.R., Lotter A.P. (1993b) Polymorphs of nitrofurantoin. 2. Preparation and X-ray crystal structures of two monohydrated forms of nitrofurantoin. *Journal of Crystallographic and Spectroscopic Research* **23**: 785-790.

Rantanen J., Yliruusi J. (1998) Determination of particle size in a fluidized bed granulator with a near infrared set-up. *Pharmaceutical and Pharmacological Community* **4**: 73-75.

Rantanen J., Lehtola S., Rämet P., Mannerma J-P., Yliruusi J. (1998) On-line monitoring of moisture content in an instrumented fluidised bed granulator with a multi-channel NIR moisture sensor. *Powder Technology* **99**: 163-170.

Rantanen J., Antikainen O., Mannerma J-P., Yliruusi J. (2000) Use of near-infrared reflectance method for measurement of moisture content during granulation. *Pharmaceutical Development and Technology* **5**: 209-217.

Rantanen J., Wikström H., Turner R., Taylor L. S. (2005) Use of in-line near-infrared spectroscopy in combination with chemometrics for improved understanding of pharmaceutical processes. *Analytical Chemistry* **77** (2): 556-563.

Rantanen J. (2007) Process analytical applications of Raman spectroscopy. *Journal of Pharmacy and Pharmacology* **59**: 147-159.

Reich G. (2005) Near-infrared spectroscopy and imaging: Basic principles and pharmaceutical applications. *Advanced Drug Delivery Reviews* **57**: 1109-1143.

Räsänen E., Rantanen J., Jørgensen A. C., Karjalainen M., Paakkari T., Yliruusi J. (2001) Novel identification of pseudopolymorphic changes of theophylline during wet granulation using near infrared spectroscopy. *Journal of Pharmaceutical Sciences* **90** (3): 389-396.

Räsänen E., Sandler N. (2007) Near infrared spectroscopy in the development of solid dosage forms. *Journal of Pharmacy and Pharmacology* **59**: 147-159.

Rodrigues L. O., Alves T. P., Cardoso J. P., Menezes J. C. (2006) Improving drug manufacturing with process analytical technology. *IDrugs* **9**: 44-48.

Roggo Y., Jent N., Edmond A., Chalus P., Ulmschneider M. (2005) Characterising process effects on pharmaceutical solid forms using near-infrared spectroscopy and infrared imaging. *European Journal of Pharmaceutics and Biopharmaceutics* **61**: 100-110.

Romero-Torres S., Perez-Ramos J. D., Morris K. R., Grant E. R. (2005) Raman spectroscopic measurement of tablet-to-tablet coating variability. *Journal of Pharmaceutical and Biomedical Analysis* **38** (2): 270-274.

Romero-Torres S., Perez-Ramos J. D., Morris K. R., Grant E. R. (2006) Raman spectroscopy for tablet coating thickness quantification and coating characterization in the presence of strong fluorescent interference. *Journal of Pharmaceutical and Biomedical Analysis* **41** (3): 811-819.

Ruotsalainen M., Heinämäki J., Rantanen J., Yliruusi J. (2002) Development of an automation system for a tablet coater. *AAPS PharmSciTech* **2**: article 14.

Savitzky A., Golay M. J. E. (1964) Smoothing and differentiation of data by simplified least squares procedures. *Analytical Chemistry* **36** (8): 1627- 1639.

Scafi S. H. F., Pasquini C. (2001) Identification of counterfeit drugs using near-infrared spectroscopy. *Analyst* **126** (12): 2218-2224.

Siesler H. W. (2002) Introduction. Near-infrared spectroscopy. Principles, instruments, applications. H.W. Siesler, Editor. Weinheim, WILEY-VCH Verlag GmbH, pp. 1-10.

Stein H. H., Ambrose J. M. (1963) Near infrared method for determination of water in aluminium aspirin. *Analytical Chemistry* **35**: 550-552.

Spencer J. A., Jefferson E.H., Hussain A.S., Newnham D., Lo T. (2007) Tablet content analysis using terahertz transmission spectroscopy. *Journal of Pharmaceutical Innovation* **2**: 18-22.

Stephenson G. A., Stowell J. G., Toma P. H., Pfeiffer R. R., Byrn S. R. (1997) Solid-state investigations of erythromycin A dihydrate: Structure, NMR spectroscopy, and hygroscopicity. *Journal of Pharmaceutical Sciences* **86** (11): 1239-1244.

Stephenson G. A., Groleau E. G., Kleemann R. L., Xu W., Rigsbee D. R. (1998) Formation of isomorphic desolvates: Creating a molecular vacuum. *Journal of Pharmaceutical Sciences* **87** (5): 536-542.

Stephenson G. A. (2005) Applications of X-ray powder diffraction in the pharmaceutical industry. *The Rigaku Journal* **22** (1): 2-15.

Strachan C. J., Rades T., Newhamn D. A., Gordon K. C., Pepper M., Taday P. F. (2004) Using terahertz pulsed spectroscopy to study crystallinity of pharmaceutical materials. *Chemical Physics Letters* **390**: 20-24.

Strachan C. J., Taday P. F., Newhamn D. A., Gordon K. C., Zeitler J. A., Pepper M., Rades T. (2005) Using terahertz pulsed spectroscopy to quantity pharmaceutical polymorphism and crystallinity. *Journal of Pharmaceutical Science* **94** (4): 837-846.

Strachan C. J., Ho L., Zeitler J. A., Rades T., Gordon K. C., Rantanen J. (2006) Terahertz applications for the analysis of solid dosage forms. *Pharmaceutical Technology Europe* November 2006: 27-33.

Taday P. F. (2004) Applications of terahertz spectroscopy to pharmaceutical sciences. *Philosophical Transactions of the Royal Society A* **362**: 351-364.

Taday P. F., Newnham D. A. (2004) Technological advances in terahertz pulsed systems bring far-infrared spectroscopy into the spotlight. *Spectroscopy Europe* **16** (5): 20-24.

Taylor L. S., Langkilde, F. W. (2000) Evaluation of solid-state forms present in tablets by Raman spectroscopy. *Journal of Pharmaceutical Sciences* **89**: 1342–1353.

Taylor L. S., Langkilde, F. W., Zografi G. (2001) Fourier transform Raman spectroscopic study of interaction of water vapour with amorphous polymers. *Journal of Pharmaceutical Sciences* **90**: 888-901.

Tenhunen J., Sjöholm K., Pietila K., Home S. (1994) Determination of fermentable sugars and nitrogenous compounds in wort by nearinfrared and midinfrared spectroscopy. *Journal of the Institute of Brewing* **100** (1): 11-15.

Tian F., Zeitler J. A., Strachan C. J., Saville D. J., Gordon K. C., Rades T. (2006) Characterising the conversion kinetics of carbamazepine polymorphs to the dehydrate in aqueous suspension using Raman spectroscopy. *Journal of Pharmaceutical and Biomedical Analysis* **40**: 271-280.

Vyazovkin S., Dranca I. (2005) Probing beta relaxation in pharmaceutically relevant glasses by using DSC. *Pharmaceutical Research* **23** (2): 422-428.

Wang Z. Z., Wang J. K., Dang L. P. (2006) Thermal, phase transition and spectral studies in erythromycin pseudopolymorphs: dihydrate and acetone solvate. *Crystal Research and Technology* **41** (12): 1219-1225.

Wikström H., Marsac P., Taylor L. S. (2005) In-line monitoring of hydrate formation during wet granulation using Raman spectroscopy. *Journal of Pharmaceutical Sciences* **94**: 209-219.

Wildfong P. L., Samy A-S., Corfa J., Peck G. E., Morris K. R. (2002) Accelerated fluid bed drying using NIR monitoring and phenomenological modelling: Method assessment and formulation stability. *Journal of Pharmaceutical Sciences* **91** (3): 631-639.

Wold H. (1966) Estimation of principal components and related models by iterative least squares. Multivariate Analysis, P.R. Krishnaiaah, Editor. New York: Academic Press, pp. 391-420.

Wold S., Martens H., Wold H. (1983) The multivariate calibration problem in chemistry solved by the PLS method. *Proc. Conference on Matrix Pencils*, Lecture Notes in Mathematics. A. Ruhe & B. Kastrøm, Editors. Springer Verlag, Heidelberg, pp. 286-293.

Wold S., Sjöström M., Eriksson L. (2001) PLS-regression: a basic tool of chemometrics. *Chemometrics and Intelligent Laboratory Systems* **58** (2): 109-130.

Woodward R. M., Wallace V. P., Arnone D. D., Linfield E. H., Pepper M. (2003) Terahertz pulsed imaging of skin cancer in the time and frequency domain. *Journal of Biological Physics* **29**: 257-261.

Workman J. J. (1999) Review of process and non-invasive near-infrared and infrared spectroscopy: 1993-1999. *Applied Spectroscopy Reviews* **34** (1-2): 1-89.

Workman J. J. (2000) Handbook of organic compounds: NIR, IR; Raman and UV-Vis spectra featuring polymers and surfactants, Volume 1. Academic press.

Workman J. J. (2001) Infrared and Raman spectroscopy in paper and pulp analysis. *Applied Spectroscopy Reviews* **36** (2-3): 139-168.

Workman J. J., Koch M., Veltkamp D (2007) Process analytical chemistry. *Analytical Chemistry* **79**: 4345-4364.

Yoon W. L., Jee R. D., Moffat A. C. (1998) Optimisation of sample presentation for the near-infrared spectra of pharmaceutical excipients. *Analyst* **123** (5): 1029-1034.

Yu L., Reutzel S. M., Stephenson G. A. (1998) Physical characterization of polymorphic drugs: an integrated characterization strategy. *Pharmaceutical Science & Technology Today* **1** (3): 118-127.

Yu L. X., Lionberger R. A., Raw A. S., D´Costa R., Wu H., Hussain A. S. (2004) Applications of process analytical technology to crystallization processes. *Advanced Drug Delivery Reviews* **56** (3): 349-369.

Zhang G. G. Z., Law D., Schmitt E. A., Qiu Y. (2004) Phase transformation considerations during process development and manufacture of solid oral dosage forms. *Advanced Drug Delivery Reviews* **56**: 371-390.

Zeitler J. A., Shen Y., Baker C., Taday P. F., Pepper M., Rades T. (2007a) Analysis of coating structures and interfaces in solid oral dosage forms by three

dimensional terahertz pulsed imaging. *Journal of Pharmaceutical Sciences* **96** (2): 330-340.

Zeitler J. A., Taday P. F., Newnham D. A., Pepper M., Gordon K. C., Rades T. (2007b) Terahertz pulsed spectroscopy and imaging in the pharmaceutical setting – a review. *Journal of Pharmacy and Pharmacology* **59**: 209–223.

Zeitler J. A., Taday P. F., Pepper M., Rades T. (2007c) Relaxation and crystallization of amorphous carbamazepine studied by terahertz pulsed spectroscopy. *Journal of Pharmaceutical Sciences* **96** (10): 2703-2709.